Chapter 7

Linear Friction Based Processing Technologies for Aluminum Alloys: Surfacing, Stir Welding and Stir Channeling

Pedro Vilaça, João Gandra and Catarina Vidal

Additional information is available at the end of the chapter

http://dx.doi.org/10.5772/52026

1. Introduction

The friction based processing technologies encloses some of the most significant solid state manufacturing technologies for producing structural components in aluminium alloys. In the present chapter three processes will be depicted: i) Friction Surfacing (FS); ii) Friction Stir Welding (FSW) and iii) Friction Stir Channeling (FSC). These processes covers a large range of applications and share the characteristic of being a machine tool based processes having one rotating tool that travels over the surface of the components to be processed.

The three processes addressed in this chapter: FS, FSW and FSC are of major importance when considering the manufacturing of aluminium alloy. This statement can be justified considering the fact: i) aluminium alloys are one of the most relevant material group in engineer applications, and ii) aluminium alloys are particularly suitable for being solid state processed by most of the friction based manufacturing technologies. Actually, the zone undergoing direct mechanical processing goes over a severe thermo-physical cycle resulting in dynamic recrystallization and consequent grain refinement and homogeneous fine distribution of hardening particles [1]. Therefore the processed zone of aluminium alloys typically presents benefits when compared with original pre-processed condition [2,3].

The Figure 1 presents the technological interrelations of the three processes addressed in this chapter within the scope of the friction based manufacturing technologies.

On all the friction based manufacturing technologies a viscoplasticised solid state region is generated and processed into a new shape and properties. This region whilst remaining solid presents a three-dimensional material flow pattern almost as a liquid enabling easy mix-

ing and blending between different materials. This phenomenon is generally referred to as the "third-body region" concept [4].

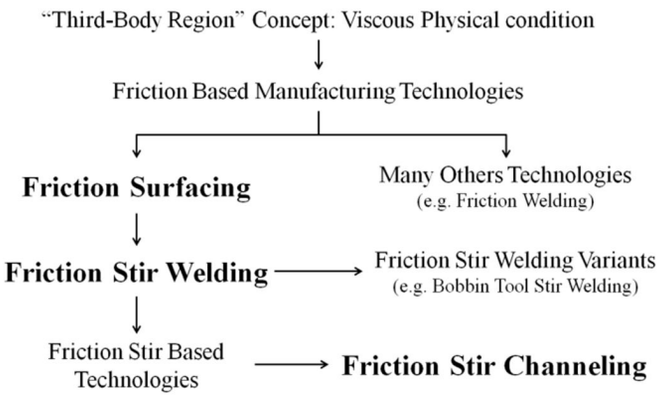

Figure 1. Friction Surfacing (FS), Friction Stir Welding (FSW) and Friction Stir Channeling (FSC) on the scope of the linear friction based manufacturing technologies.

In particularly for aluminium alloys this "third-body region" is characterized mechanically by a relatively low flow stress and by temperatures above recristalization temperature and below melting temperature of material. In the solid state processes governed exclusively by the introduction of mechanical energy (as it happens in friction based processing technologies), the heat is generated by friction dissipation during deformation at contacting interfaces and internally during material flow. Because the heat generated by friction dissipation tends to zero as the material gets near the fusion temperature the maximum temperature achieved within processed zone is physically limited by the fusion temperature and thus all the deformation is restricted to solid state condition.

One relevant property of the "third-body region" is to easily produce strong bonds at the interface with other similar solid state flowing material or even with material surfaces undergoing less severe deformation, e.g., elasto-plastic deformation. The solid state joining mechanisms involving the "third-body region" at temperatures well above recrystallization temperature are mainly diffusion, but approximation to interatomic equilibrium distances can also be found for lower temperature and higher pressure conditions at the joining interface. Thus, the "third-body region" is frequently used for promoting joining of similar and dissimilar materials in the various friction welding variants. This "easy to join" property is also used in other manufacturing technologies based on this "third-body region", e.g., extrusion of close hollow shapes where separate extruded components are joined together before exiting the dies.

The FS was firstly patented in 1941 [5] and is nowadays a well-established technology that applies one consumable tool to produce many possible combinations of coatings over a substrate. The FS is one of the many solutions developed based on the concepts of the friction manufacturing technology and the extension of its concepts gave rise to one very significant development in the history of welding technology: The FSW process that was firstly patented in 1991 [6]. The FSW is a process for joining components, using a non-consumable tool,

http://dx.doi.org/10.5772/52026

with a suitably profiled shoulder and probe. FSW can be regarded as an autogenous keyhole welding technique in the solid-phase. The FSW technology has been subjected to the most demanding quality standard requirements and used in challenging industrial applications over a wide range of structural and non-structural components mainly in aluminium alloys. The disruptive character of the FSW process is emphasized by the numerous technic-scientific papers and patents published and the several friction stir based technologies that are being invented. The FSC was proposed for the first time in 2005 as a method of manufacturing heat exchanging devices [7] and is one of the most promising innovations based on the friction stir concepts with many industrial applications, some of them will be depicted in this chapter. The FSC uses a non-consumable tool to open channels along any path, shape and depth in monolithic aluminium alloys components.

There are friction based manufacturing technologies, such as, FSW where material flow within the "third-body region" is three-dimensionally enclosed and thus the process is flashless. In FSW the "third-body region" is constrained at top and bottom by the system: shoulder + anvil, and at the sides by the cold base material. But there are others friction based manufacturing technologies where the "third-body region" is open (or not fully constrained) and bulk flash is generated, e.g., FS. For the case of FSC one other intermediate condition is present: although the "third-body region" is three-dimensionally enclosed some of the inner material from the "third-bodyregion" is forced out by the tool features, producing an amount of flash volume correspondent to the volume of the inner channel produced. These conditions are depicted in Figure 2.

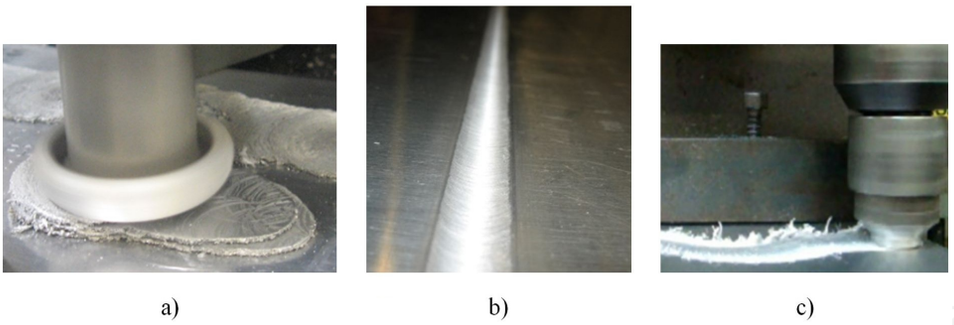

Figure 2. Sample of finishing condition of friction based manufacturing technologies: a) Flash produced during FS due to unconstrained "third-body region"; b)Flashless condition of as-welded FSW due to complete enclosure of the material flow within the "third-body region"; c) Flash forced out of processing zone by the tool features during FSC.

The cost effectiveness of the three friction based manufacturing technologies addressed in this chapter is very promising: i) All the processes are environmentally friendly solutions, ii) Because of the low heat input demanded for the solid state processing all these solutions have high energy efficiency when compared with alternative/concurrent solutions; iii) The health and safety impact for human operators is insignificant due to no fumes emission and residual radiation and equipment with low operational hazards; iv) Since there are no consumables for FSW and FSC, and the only consumable in FS is the rod to be deposited over the substrate, any initial investment in the equipment typically have an early breakeven

point, when compared with alternative/concurrent solutions; v) All these technologies are easy to automate with good repeatability of the results and high levels of quality assurance.

The Table 1 establish the composition and temper of the aluminium alloys involved in the several applications of the friction based manufacturing technologies addressed in this chapter. This Table 1 is intended to be used as support for the analysis of the results presented along the chapter.

Material	*Composition (weight%)*										*Temper*
	Al	**Cu**	**Mg**	**Si**	**Zn**	**Mn**	**Fe**	**Cr**	**V/Ti**	**Other, each**	
AA1050-O	≥99.5	≤0.05	≤0.05	≤0.25	≤0.05	≤0.05	≤0.40		≤0.05/	≤0.03	Annealed
AA2024-T3	remain	3.80 to 4.90	1.20 to 1.80	≤0.50	≤0.25	0.30 to 0.90	≤0.05	≤0.10	/≤0.15	0.05	Solution heat treated, cold worked, and naturally aged to a substantially stable condition
AA5083-H111	remain	≤0.10	4.0 to 4.90	≤0.40	≤0.25	≤0.40 to 1.0	≤0.40	0.05 to 0.25	/≤0.15	≤0.05	Small degree of strain-hardening only
AA6061-T4	remain	0.15 to 0.40	0.80 to 1.20	0.40 to 0.80	≤0.25	≤0.15	≤0.70	0.04 to 0.35	/≤0.15	≤0.05	Solution heat treated and naturally aged to a substantially stable condition
AA6082-T6	remain	≤0.10	0.60 to 1.20	0.70 to 1.30	≤0.20	0.40 to 1.0	≤0.50	≤0.25	/≤0.10	≤0.05	Solution heat treated and artificially aged
AA7178-T6	remain	1.60 to 2.40	2.40 to 3.10	≤0.40	6.30 to 7.30	≤0.30	≤0.50	0.18 to 0.28	/≤0.20	≤0.05	Solution heat treated and artificially aged

Table 1. Composition and temper designation of the aluminium alloys referenced within the present chapter.

2. Friction surfacing

2.1. Fundaments of the process

Friction surfacing (FS) is a solid state process used for the production of metallic coatings with metallurgical characteristics typical from hot forging operations. The process involves rubbing a rotating consumable rod (Figure 3a) against a substrate under an applied axial load. Heat generated by frictional dissipation promotes the viscoplastic deformation at the tip of the rod (Figure 3b).

As the consumable travels along the substrate (Figure3c), the viscoplastic material at the vicinity of the rubbing interface is transferred over onto the substrate surface, while pressure and heat conditions trigger a inter diffusion process that soundly bonds it. As the consuma-

http://dx.doi.org/10.5772/52026

ble rod material undergoes a thermo-mechanical process, a fine grained microstructure is produced by dynamic recrystallization. As shown in Figure 3d, FS enables the production of a continuous deposit from the progressive wear of the consumable rod. However, the coating cross section presents poorly bonded edges on both advancing and retreating sides, which are closely related to process parameters. The process is also characterized by the constant generation of a revolving flash of viscoplastic material at the rod tip, responsible for a smooth mushroom-shaped upset on the consumable rod [8,9].

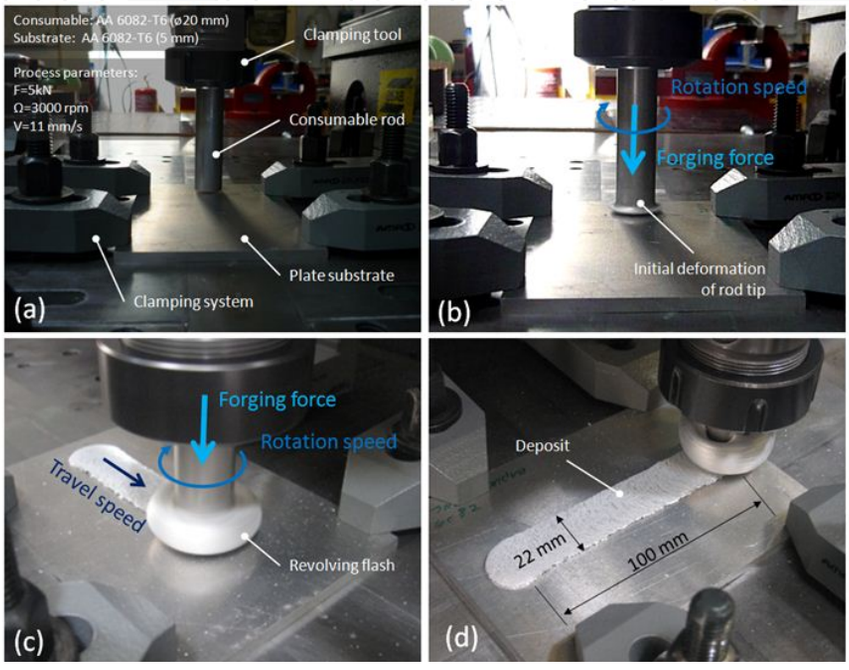

Figure 3. Deposition of AA6082-T651 aluminium alloy by friction surfacing. a) Experimental setup; b) Initial plunging phase; c) Deposition; d) Coating produced.

2.2. General features

The Figure 4 presents a cross section macrograph of both rod and coating, depicting the gradual transformations that the consumable material undergoes as it is deposited, as well as, the flash developed. Consumable rod microstructure is depicted in Figure 4a, presenting an anisotropic grain structure aligned along the rod extrusion direction. The hot working of the consumable rod tip and the deposit generates heat which is conducted along the consumable, pre-heating the material and enabling its plastic deformation by the colder material layers above in a compression/torsion process. Consumable rod heat affected microstructures presenting some precipitate coarsening and grain growth can be seen in Figure 4b, while evidences of plastic deformation are depicted in Figure 4c and d. The combination of plastic deformation and heat generation leads to a dynamic recrystallization which processes the material into a viscoplastic state with the nucleation and growth of a new set of undeformed grains (Figure 4e and f). FS enables the thermo-mechanical processing of the consumable material into a new metallurgical state.

Since this viscoplastic region is pressed against the substrate at temperatures approximately 50-90 % of the melting point, a diffusion bonding process takes place and a deposit of hot-worked consumable rod material is produced. Plastic deformation and friction can disrupt the relatively brittle oxide layers, establishing metal-to-metal contact and enabling the joining process [10]. The low heat input inherent to the FS process delivered locally over the substrate of an high thermal conductor material as the aluminium alloys are, will result in high cooling rates of the thermomechanically processed zone. Considering that fast cooling prevent grain growth, this may be the reason for the typical fine equiaxial recrystallized microstructure of the deposited material, depicted in Figure 4g. Heat is lost mainly by conduction to the substrate, originating the heat affected zone. A fully bonded interface can be seen in Figure 4h.

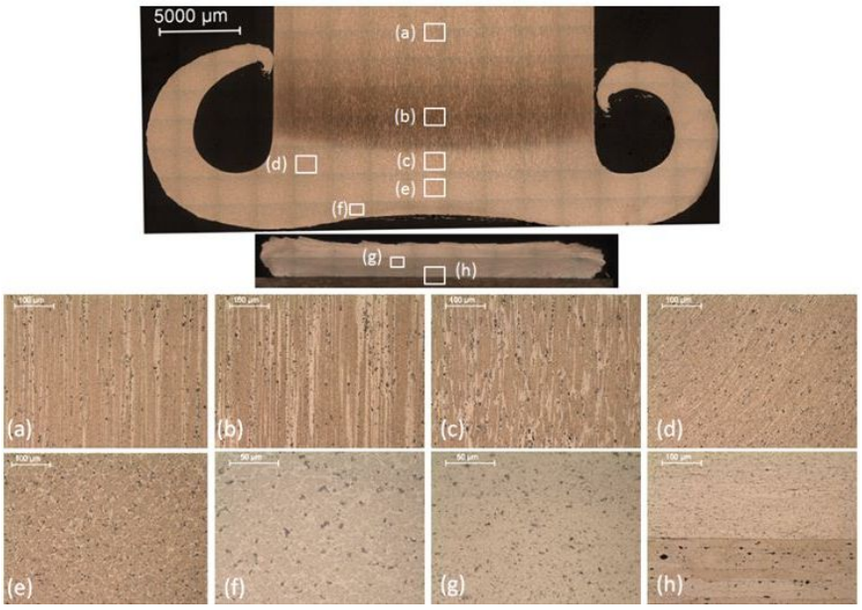

Figure 4. Microstructural transformations during the FS of AA6082-T6 over AA2024-T3.a) Consumable base material; b) Heat affected zone; c) Compression-driven TMAZ; d) Torsion-driven TMAZ; e-f) Fully recrystallized microstructure; g) Deposited material; h) Bonding interface.

The Figure 5 illustrates a proposed model for the global thermal and mechanical processes involved during friction surfacing, based on the metallurgical transformations described above. The speed difference between the viscoplastic material, which is rotating along with the rod at Vxy, and the material effectively joined to the substrate (Vxy = 0), causes the deposit to detach from the consumable. This viscous shearing friction between the deposit and the consumable is the most significant heat source in the process.

Since the highly plasticized material at the lower end is pressed without restraint, it flows outside the consumable diameter, resulting into a revolving flash attached to the tip of the consumable rod and poorly bonded coating edges. Unbonded regions are also related to the higher tangential speed at which the material flows at the outer radius of the consumable rod, because the relative speed between the deposit and the substrate shears the bonding interface and disrupts the ongoing diffusion bonding process. Nevertheless, flash and un-

http://dx.doi.org/10.5772/52026

bonded regions play an important role as temperature and pressure boundary conditions for the joining process.

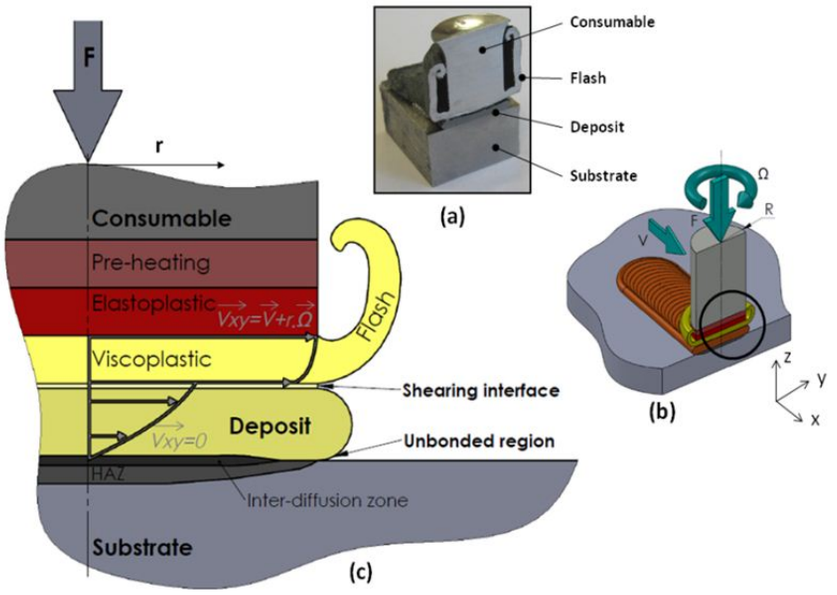

Figure 5. Thermo-mechanics of friction surfacing.a) Sectioned consumable; b) Process parameters and c) Thermo-mechanical transformations and speed profile. Nomenclature: F – forging force; Ω – rotation speed; V -travel speed; Vxy – rod tangential speed in-plan xy given by composition of rotation and travel movements.

2.3. Parameters of the process

Coatings are evaluated based on thickness, width and bond strength/extension which depend on controllable process parameters, such as, i) forging force; ii) rotation speed and iii) travel speed. Substrate thickness, rod diameter and material properties define the thermo-mechanical system thus determining process parameters:

- Forging force - improves bonding extension and results in wider and thinner deposits. However, excessive loads result in non-uniform deposition with a depression at the middle of the pass due to material expelling from the region beyond consumable rod diameter. Insufficient forging forces result in poor consolidated interfaces;
- Rotation speed - influences the bonding quality and coating width. While lower to intermediate rotation speeds enhance bonding quality, higher rotation speeds produce a more flat and regular deposit, with a more effective forging effect shaping the coating;
- Travel speed - strongly influences coating thickness and width, since it determines the rate at which material is deposited. As such, higher travel speeds result in thinner deposits. Faster travel speeds lead to shorter heat exposure periods, resulting in less grain growth and finer microstructures. Thinner deposits also cool more rapidly. The substrate heat affected zone decreases for higher travel speeds. Bonding at coating edges deteriorates for faster travel speeds;

- Tilt angle - A small tilting the consumable rod, in less than 3, has proven to reduce the unbounded extension of the deposit at the coating edges, by enabling a gradual increase of forging pressure applied by the consumable rod on the substrate, from the tip to the tail zone being thermomechanically processed, at each instant.

The Table 2 depicts the range of process parameters best suited for the friction surfacing of AA6082-T6, using 20 mm diameter consumable rods over various aluminium alloy substrate plates and resulting coating thickness, width and bonded width. In general, the fully bonded width of the deposit rarely exceeds the diameter of the consumable rod used, while the coating width extends beyond it, as evidenced by Figure 4.

Materials		Process parameters				Coating characteristics		
Consumable rod	Plate substrate	Forging force [kN]	Rotation speed [rpm]	Travel speed [mm/s]	Tilt angle [°]	Thickness [mm]	Deposit width [mm]	Bonded width [mm]
AA6082-T6 (20 mm)	AA2024-T3 AA7178-T6 AA5083-H111 AA1050-O	5 to 7	2500 to 3000	6 to 12	0 to 3	1 to 2	20 to 25	15 to 20

Table 2. Typical range of process parameter in the FS of AA6082-T6 over several aluminium substrate plates.

2.4. Advantages and limitations

Being a solid state process, FS allows depositing various dissimilar material combinations. Investigations report the deposition of stainless steel, tool steel and nickel-based alloys (Inconel) on mild steel substrates, as well as, stainless steel, mild steel and inconel consumables on aluminium substrates [11,12].

FS is best suited for applications with material compatibility issues. The process involves a hot forging action, which refines significantly the microstructure of the deposited material. The deposit is inherently homogenous and has good mechanical strength. The process can be automated, providing good reproducibility and doesn't depend on operator skill [13].

Since FS is mainly based on plastic deformation, this process presents some advantages over other coating technologies based on fusion welding or heat-spraying processes. Apart from avoiding defects commonly associated to fusion and solidification mechanisms (coarse microstructures, intermetallic formation, porosities, hot cracking or inclusions, e.g., slag), the heat input in FS is minimum and localized, preventing part distortion and minimizing the heat affected zone extension and dilution. This also makes FS suitable to process thermal sensitive materials, such as, aluminium alloys. Additionally, the absence of spatter, toxic fumes and emission of radiation makes this process cleaner and environmentally friendly. The absence of fusion and fast cooling rates enable to FS in a great variety of positions [14].

http://dx.doi.org/10.5772/52026

However, FS struggles with some technical and productivity issues which contribute to a limited range of engineering applications. One of the main process disadvantages is the poor bonding at the coating edges, as post-processing operations are often required to remove them. Moreover, the generation of a revolving flash at the consumable rod tip contributes to a decrease in mass transfer efficiency, as it represents material that does not bond to the substrate. Friction surfacing enables a limited control over the deposited thickness and width, as coating geometry is determined by a very narrow range of process parameters.

2.5. Properties and applications

The FS allows the dissimilar joining of materials that would be metallurgical incompatible otherwise. It allows assembling in a single composite component, tailored material property combinations which are difficult to gather in a single monolithic material. This enables an advanced and detailed design, adjusting the required material properties according to different loading areas of a part and precluding the use of more expensive and specific materials capable of assembling all functional requirements.

Although FS has limited large-overlay capabilities, this process is ideal for localized repair and cladding. The FS has been used in the production of long-life industrial blades, wear resistant components, anti-corrosion coatings and in the rehabilitation of worn or damaged parts such as, turbine blade tips and agricultural machinery. Other applications feature the hard facing of valve seats, brake disks and tools such as punches, guillotine blades and drills. The surfacing of pipe flange contact faces, the reclamation of worn railway points and the hermetic sealing of containers has also been reported as promising applications [15,16].

The FS can be performed over a great variety of substrate configurations and along complex trajectories. Some examples of FS path case studies can be seen in Figure 6. Figure 6a displays a single FS curvilinear path, while Figure 6b depicts a continuous cylindrical build-up, as the consumable rod moves along a 3D helicoidally trajectory.

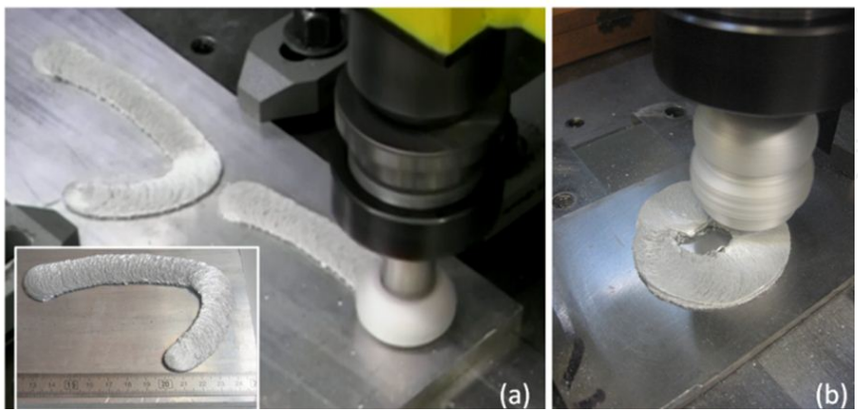

Figure 6. Examples of friction surfacing trajectories. a) Curve path; b) cylindrical build-up.

Given the rough coating surface, FS is often followed by post processing operations in order to achieve the desired geometry and surface finish. The Figure 7 depicts the milling surface

finish of a friction surfaced AA6082-T6 deposit presenting a fully bonded defect-free layer and a smooth surface finish.

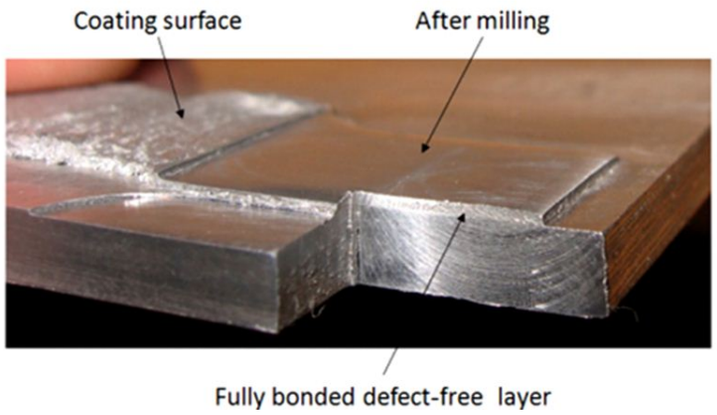

Figure 7. Surface finish by milling. FS of AA6082-T6 over AA7178-T6.

Another promising application consists on the vertical build-up of structures by performing successive fully overlapped depositions. Figure 8 depicts the manufacturing of a trapezoidal linear rail milled from the build-up of several AA6082-T6 friction surfaced passes. Figure 8d depicts the soundly bonded deposited layers, as FS allows the production of bulk layered composite materials from which parts or component features can be manufactured.

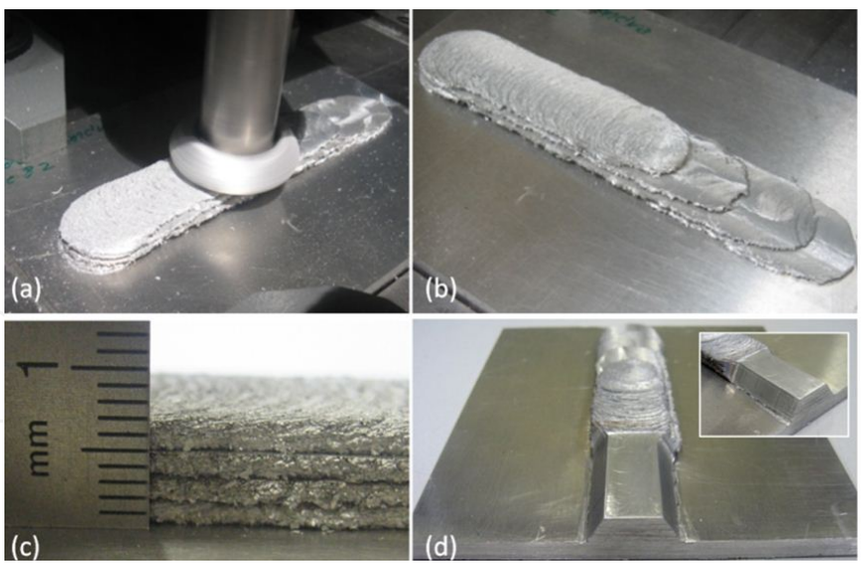

Figure 8. Build-up by friction surfacing. a) Successive deposition; b) Bulk produced from four overlapped passes; c) Detail of final thickness achieved; d) Milling of linear rail.

The mechanisms involved in friction surfacing enable an alternative process to produce surface composites, as the inherent severe plastic deformation can be used to promote the dispersion and mixture of reinforcement particles within the deposit matrix. Figure 9 depicts

http://dx.doi.org/10.5772/52026

the joining interface between an aluminium silicon carbide reinforced composite layer over an AA2024-T3 plate substrate. AA6082-T6 aluminium rods were packed with 12.3 μm silicon carbine particles and used as consumables. A uniform distribution of reinforcements was achieved as the composite layer becomes soundly bonded to the substrate. Surface hardness severely increased and gradually decreased along the thickness. By increasing the volume of reinforcements packed inside the consumable rod, higher concentration distributions can be achieved, as shown by Figure 9b.

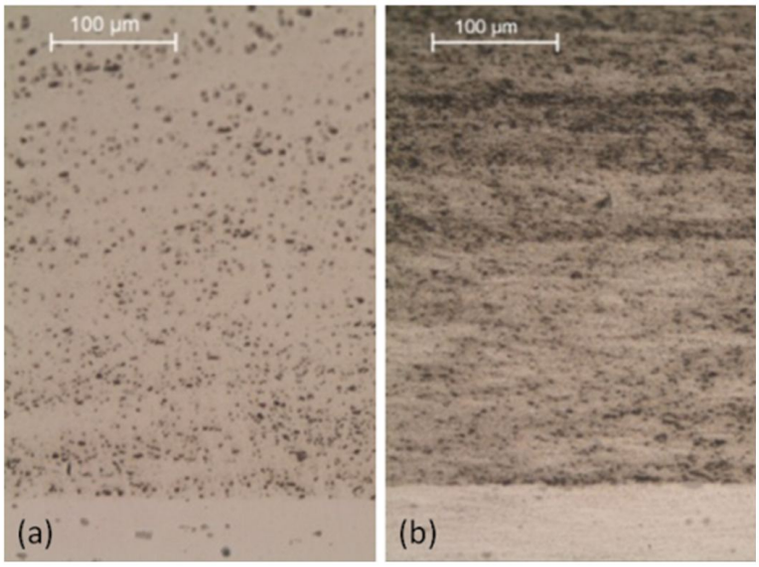

Figure 9. Joining interface of SiC reinforced AA6082-T6 coatings produced by FS over AA2024-T3 substrate.

2.6. Analytical modeling: establishment of performance analysis

Performance criteria regarding the material deposition rate and specific energy consumption were established inreference [17] for the characterization of friction surfacing, thereby contributing to establish a realistic comparison with other coating technologies.

2.6.1. Mass transfer

The Figure 4 depicts the material flow from the consumable rod to the deposit bonded to the substrate. Volumetric rod consumption rate (*CRvol*) is determined by multiplying the rod plunging speed (V_z) by its cross section area (A_r), where *r* is the rod radius (1).

$$CRvol[m^3/s] = A_r V_z = \pi r^2 V_z \quad (1)$$

Likewise, the product between the travel speed (V) and the deposited cross section area (Ad), expresses the volumetric deposition rate (DRvol) throughout the friction surfacing process (2).

$$DRvol[m^3/s] = A_d V \tag{2}$$

Considering the consumable rod material density (ϱ), CR and DR can be rewritten in order to express the mass flow, as depicted by (3) and (4).

$$CR[kg/s] = CRvol \times \varrho \tag{3}$$

$$DR[kg/s] = DRvol \times \varrho \tag{4}$$

The Figure 10 presents the effect of process parameters on deposition (*DR*) and consumption (*CR*) rates for the FS of AA6082-T6 over AA2024-T3. Deposition rates were seen to vary from 200 to 600 mm^3/s (0.5-2 g/s), increasing for higher travel speeds. The increase of rotation speed and forging force has a negative effect on *DR*.

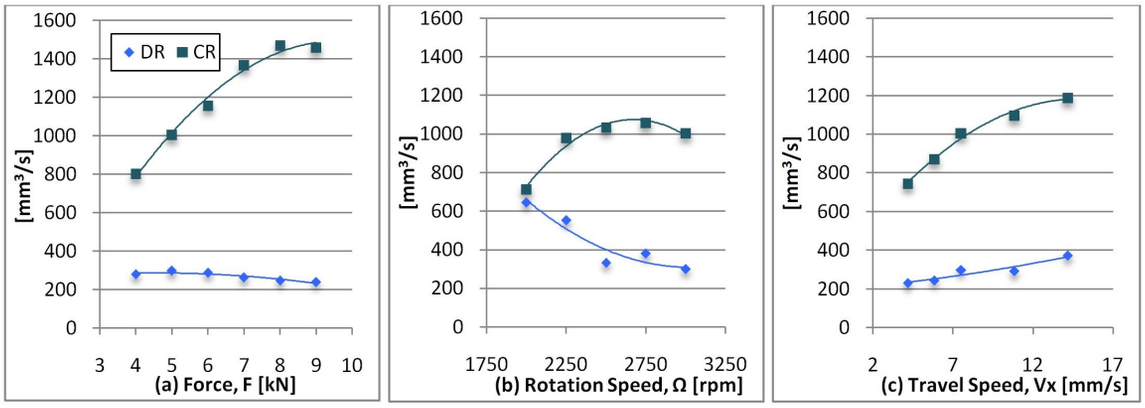

Figure 10. Effect of process parameters on deposition rate (DR) and consumption rate (CR). FS of AA6082-T6, 20 mm diameter consumable rods, over AA2024-T3 plates. Process parameters: a) Ω = 3000 rpm, V = 7.5 mm/s; b) F = 5 kN, V = 7.5 mm/s; c) F = 5 kN, Ω = 3000 rpm.

In order to determine the fraction of consumed material deposited and that is transferred to flash, a deposition efficiency ($\eta_{deposition}$) can be defined as the ratio between DR and CR via (5).

$$\eta_{deposition} = DR/CR \tag{5}$$

Due to the formation of side unbonded regions, just a part of the deposited material is effectively joined. As such, the joining efficiency ($\eta_{joining}$) is given by the ratio between the bonded width (Wb) and the maximum coating width (Wd) established in (6).

$$\eta_{joining} = W_b/W_d \tag{6}$$

Thus, the effective coating efficiency ($\eta_{coating}$) reflects the fraction of consumed rod that actually becomes bonded to the substrate and is estimated via (7) by multiplying (5) times (6):

http://dx.doi.org/10.5772/52026

$$\eta_{coating} = \eta_{deposition} \bullet \eta_{joining} = \frac{A_d v}{\pi r^2 V_z} \bullet \frac{W_b}{W_d} \quad (7)$$

Considering the process parameter range depicted in Table 2, in the FS of AA6082-T6 over AA2024-T3, maximum joining efficiency and coating efficiency reached around 82 % and 25 %, respectively. Recently research performed by the authors of the present chapter also shows that flash formation accounts 60 to 70 % of the overall consumable rod consumption.

2.6.2. Energy consumption

The mechanical power supplied by the equipment ($\dot{W}_e$) can be divided into three main contributions regarding rod rotation, $\dot{W}_r$, axial plunging, $\dot{W}_z$, and travel, $\dot{W}_x$, as established in (8).

$$\dot{W}_e[J/s] = \dot{W}_r + \dot{W}_z + \dot{W}_x = \frac{2\pi\Omega}{60}(T_1 - T_0) + F_z V_z + F_x V \quad (8)$$

T0 is the torque required to freely rotate the consumable rod without any contact friction, e.g., the torque applied by the machine to impel the prescribed rotation speed and depends on the machine mechanical design, rather than deposition process. When the machine starts to plunge the rod against the plate substrate it raises the torque from T0 to T1.

Hence, for a joining efficiency of 100%, energy consumption per deposited unit of mass (specific energy consumption, EC) is given by (9).

$$EC[J/kg] = \dot{W}_e / DR \quad (9)$$

The Figure 11 depicts the variation of power and specific energy consumption for the tested conditions. Power increases with the forging force and the travel speed, varying between 4-6 kW. The specific energy consumption computed according to equation (9) varies from 8 to 26 J/mm3 (4-10 kJ/g). Specific energy consumption increases with the forging force (Figure 11a). For high rotation speeds, although both the required power and the deposition rate drop, specific energy consumption rises, meaning that the decrease in deposition rate is more significant (Figure 11b). Excessive rotation speeds result in less joining efficiency and increased specific energy consumption per unit of mass. Despite the increase in power, specific energy consumption decreases with travel speed (Figure 11c), given a more significant improvement of deposition rate (Figure 10c). Hence, faster travel speeds allows to improve deposition rates while decreasing specific energy consumption.

Considering the present testing conditions in Table 2, the best processing conditions were achieved for a 500 kN forging force, 2500 rpm rotation speed and a 7.5 mm/s travel speed, which resulted in a specific energy consumption of 12 J/mm3 with a deposition rate of 332 mm3/s. Joining efficiency and coating efficiency was 76 % and 32 %, respectively, while flash accounted for 67 % of consumed material.

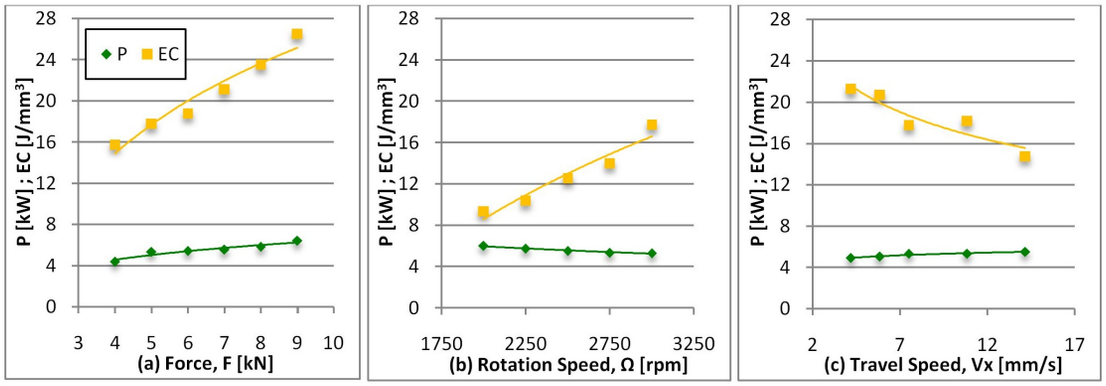

Figure 11. Effect of process parameters on friction surfacing power and specific energy consumption. FS of AA6082-T6, 20 mm diameter consumable rods, over AA2024-T3 plates. Process parameters: a) Ω = 3000 rpm, V = 7.5 mm/s; b) F = 5 kN, V = 7.5 mm/s; c) F = 5 kN, Ω = 3000 rpm.

3. Friction Stir Welding

3.1. Fundaments of the process

The FSW is a process for joining components in the solid phase, using an intermediate non consumable tool, with a suitably profiled shoulder and probe, made of material that is harder than the workpiece material being welded. FSW can be regarded as an autogenous keyhole joining technique, essentially, without the creation of liquid metal.

The rotating tool is plunged into the weld joint and forced to travel along the joint line, heating the components by interfacial and internal friction dissipation, thus producing a weld joint by extruding, forging and stirring the materials from the components in the vicinity of the tool. The basic principles of the process and some nomenclature are represented in Figure 12.

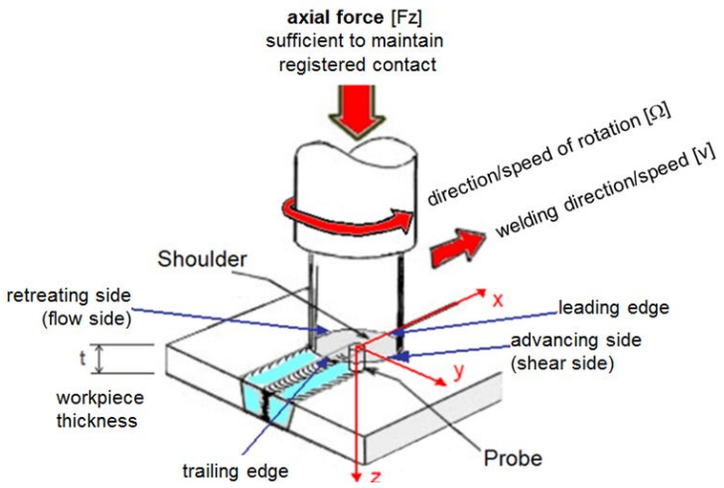

Figure 12. Representation of the main parameters and nomenclature of FSW joints.

http://dx.doi.org/10.5772/52026

The shoulder and the probe thermo mechanically soften and then separate the material being processed by the passage of the probe through the material. The material flows around the probe and is then forge welded together at the trailing edge of the probe. This separation and welding together occur continuously by backfilling from the probe and compaction/containment from the shoulder. This transient separation/rewelding operation happens during and before the trailing edge of the shoulder moves away from the processed/weldtrack. The transient "third-body region" immediately coalesces and forms a solid phase bond as the tool moves away.

The material flow within closed "third-body region" is characterized by [18, 19] :i) on the retreating side of the weld, material is displaced only backward; For any material actually in the path of the probe, the flow reverses and results in material being displaced to a position behind its original position (relative to the welding direction); iii) The material at mid-height in the advancing side near the probe is flowing all around the retreating side being left behind it original position in a kind *swiss roll* movement, that maybe the mechanism of formation of the onion rings in the nugget and iv) Material on the advancing side under the shoulder and near the periphery (but under shoulder influence) is displaced in the forward direction of welding relative to its original position.

3.2. Parameters of the process

The main FSW process parameters are the following:

- Tool geometry;
- Plunge speed and depth of probe in workpieces;
- Tool rotational speed () and direction;
- Travel Speed (V) along the joint line;
- Axial load, Fz;
- Dwell time at start of the weld;
- Clamping system (stiffness, precision and material of the anvil, for easy extraction of workpieces);
- Tilt and side tilt angles;
- Control during plunge, dwell and weld periods: Force control (Fz) *versus* position control;
- Preheating/interpass temperature of workpieces;
- Weld pitch ratio, see equation (10). Varying the weld pitch ratio changes the heat input from the frictional internal and interfacial energy and some effects in the weld region behaviour can be predictedThe weld pitch ratio provides a possible classification for the flow pattern within the third-body zone [1, 20]. For aluminium alloys it is usual to consider the value of weld pitch ratio = 4 as intermediate condition. For weldpitch ratio higher than 4 there is hot condition and for weldpitch ratio smaller than 4 there is cold condition.

Concerning the influence of the hot-to-cold conditions in the metallurgical features of a FSW weld joint, the classification is established in (11), where the HAZ and TMAZ are described in §3.3.

$$\text{weld pitch ratio } [\text{rev/mm}] = \frac{\Omega[\text{rpm}]}{\text{v}[\text{mm/min}]} \tag{10}$$

$$\text{FSW Classification:} \begin{cases} Hot \Leftrightarrow \begin{cases} \uparrow \Omega \\ \downarrow v \end{cases} \Rightarrow \begin{cases} \uparrow HAZ \\ \downarrow TMAZ \end{cases} \\ Cold \Leftrightarrow \begin{cases} \downarrow \Omega \\ \uparrow v \end{cases} \Rightarrow \begin{cases} \downarrow HAZ \\ \uparrow TMAZ \end{cases} \end{cases} \tag{11}$$

3.3. General metallurgical, hardness, mechanical and corrosion resistance features

During the FSW process, the material undergoes intense plastic deformation at elevated temperature, as a rule resulting in the generation of fine and equiaxed re-crystallized grains. This fine microstructure produces good mechanical properties in friction stir welds. Better quality joints are associated with intense three-dimensional material flow. Thus for aluminium alloys is more easy to obtain high levels of quality and reproducibility when welding bigger thicknesses than when welding small thickness, e.g., equal or less than 1 mm, where the material flow tends to be bi-dimensional and the stirring of the materials is consequently poorer [21,22].

The main zones in a FSW joint with distinct metallurgical properties are: i) the thermomechanically affected central zone (TMAZ) that includes the dynamically recrystallized zone (nugget); ii)The heat affected zone (HAZ) and iii) The unaffected parent material or base material (BM).These different zones result from the combined application of mechanical energy and heat energy from frictional dissipation. The typical characteristics of each of these zones for aluminium alloys are the following:

- The BM is the region that was unaffected by the FSW process;
- The HAZ is only affected by the heat energy and presents typically some slight coalescence of grain relatively to the original grain size but is subjected to internal point and linear defects rearrangements. Thus, for the heat treatable wrought aluminium alloys the HAZ may presents some reduction in the distribution of precipitates at grain boundaries;
- The TMAZ grain maintains the characteristics of the HAZ however the grain presents increased deformation as they get close to the interface with the nugget. This fact results from the influence of the material flow prescribed by the movement of the tool and the relatively high maximum temperature reached in this zone;
- The nugget is the region of the TMAZ undergoing dynamic recrystallization with grain size refined and homogenized. The TMAZ/nugget interface enhances the significant dif-

http://dx.doi.org/10.5772/52026

ference between the structure of initial grain and the equiaxial grain resultant of the dynamical recrystallisation process with fine dispersion of the precipitates in the solid solution.

The typical metallurgical structures present in the processed zone of friction stir welds are established and classified in Figure 13 for a heat treatable aluminium alloy (AA2024-T3) and in Figure 14 for a non-heat treatable aluminium alloy (AA5083-H111).

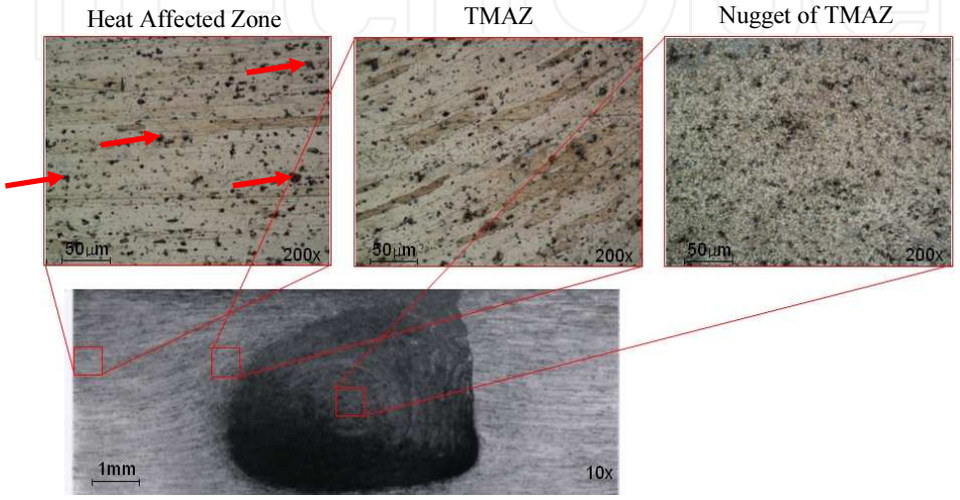

Figure 13. Metallographic analysis of a FSW of AA2024-T3 (thickness = 4.8 mm), Ω = 1120 rpm, v = 320 mm/min. The arrows in the HAZ detail are identifying some of the several precipitates.

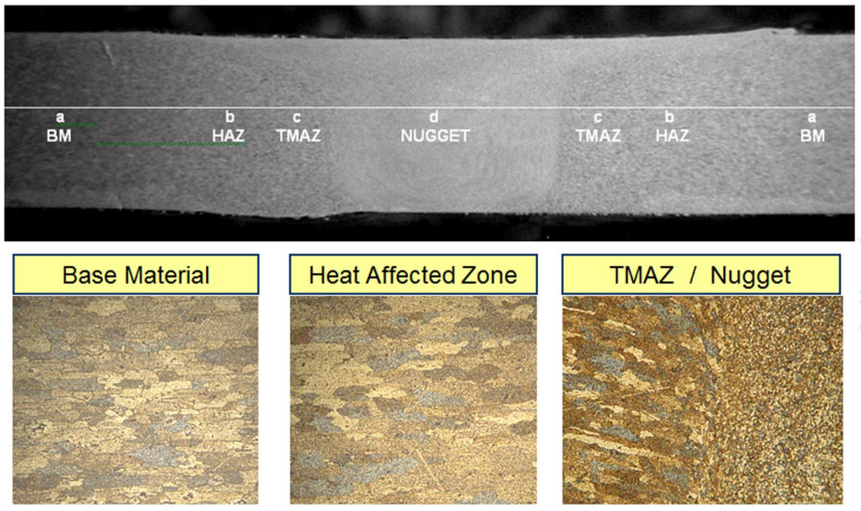

Figure 14. Metallographic analysis of a FSW of AA5083-H111 (thickness = 4.0 mm), Ω = 1120 rpm, v = 320 mm/min.

In Figure 15, it is possible to analyze some relevant characteristics, e.g.: i) relative location of the centre of the nugget; ii) width of the nugget at the centre and iii) width of the nugget at the root of the weld. This last dimension is very relevant in the quality assessment of the

FSW joints because a correct processing of the root of the joint is mandatory to avoid defects located at the root of the bead which are always important [23].

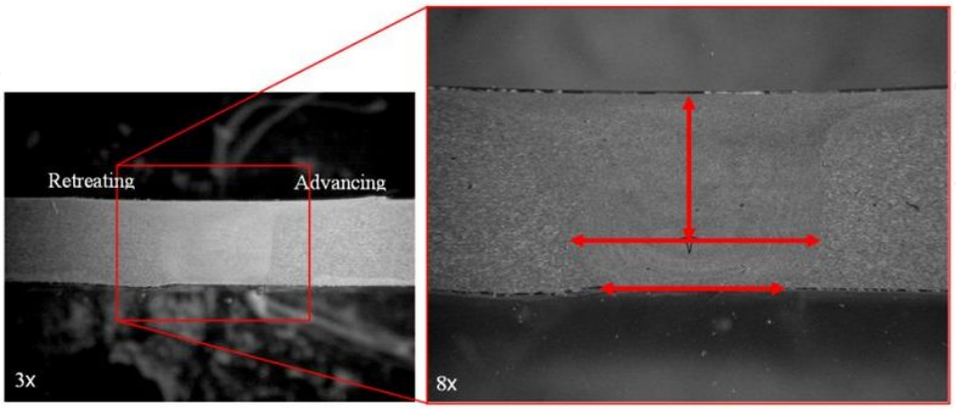

Figure 15. Relevant geometrical characteristics on a metallographic analysis of a FSW cross-section.

The Figure 16 depicts the effective location of the real slip interface which is within the material and not at the top surface in direct contact with the shoulder. In fact, there is a layer (with a thickness 10 μm) of material bellow the shoulder that is dragged to rotate along with the rotating shoulder. This phenomenon is due to the adhesion of the material to the shoulder. Even for very low friction coefficients, the contact pressures are high and the frictional force overcomes the flow stress of the workpieces material. It should also be noticed that the real slip interface is increasingly evident, as it progresses from the center to the periphery of the weld bead, in accordance with the increase of linear speed of the rotating shoulder for higher radius.

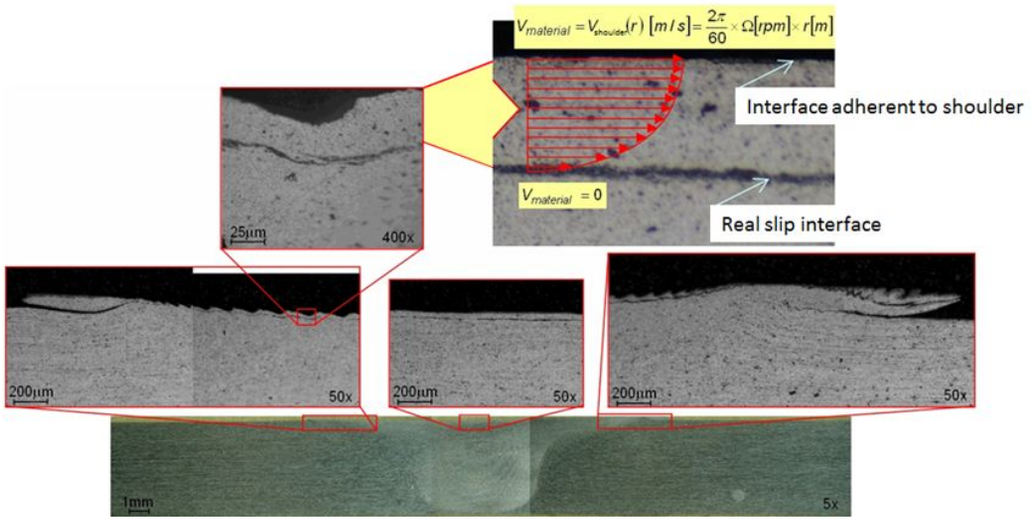

Figure 16. Superficial layer of weld bead material in contact with shoulder that is dragged to rotate along with the shoulder generating a real slip interface about 10μm within the material.

http://dx.doi.org/10.5772/52026

From the Figure 17 showing the behavior of the non-heat treatable alloys it is possible to conclude about the increased hardness of weld bead and heat affected zones when compared with base material. Because these alloys are very sensitive to strain hardening the increase is most significant in all the TMAZ with emphasis for the nugget zone [23,24].

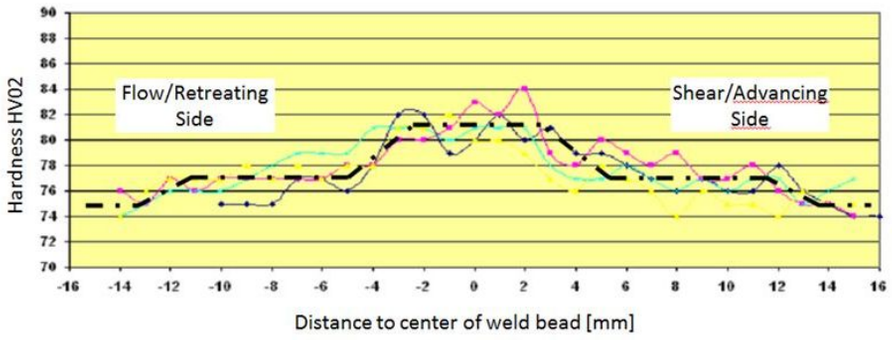

Figure 17. Typical hardness profile for the non-heat treatable wrought aluminium alloys (AA5083-H111; thickness: 4mm).

In Figure 18 it is possible to conclude about the typical location of the global minimum value of the harness field located in the interface between the HAZ and the TMAZ. Along the HAZ there is typically a local minimum due to over ageing. Depending on the pattern of material flow during the FSW… for more cold conditions the minimum value at the flow side (retreating side) is smaller than at the shear side (advancing side). For FSW under more hot conditions the minimum values in both sides of the weld bead have more identical values [1,24].

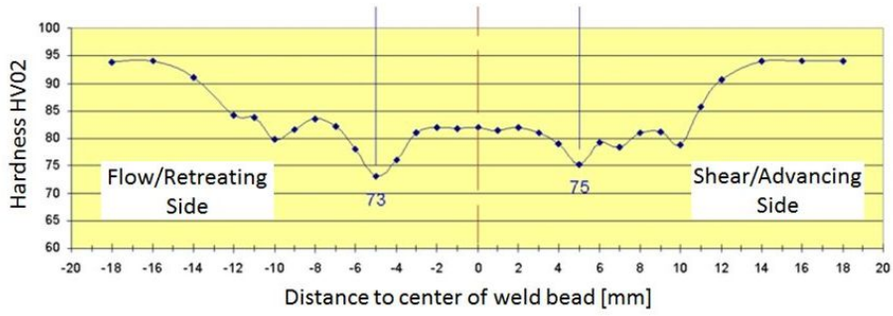

Figure 18. Typical hardness profile for the heat treatable wrought aluminium alloys (AA6061-T4; thickness: 4.8mm).

The hardness profile enables a reliable assessment of the static mechanical resistance of the joints but the fatigue resistance is more dependent on the geometric characteristics of the weld bead at the top and bottom surfaces and eventual internal defects both volumetric or layers/alignment of second phase particles or oxides, e.g., lack of penetration (LOP) root defects [25]. The fracture mechanism of FSW specimens under fatigue load is mainly determined by the size of the defect at the root of weld bead. For the FSW beads in as welded

condition the higher critical level of the root defect always resulted in less number of cycles when compared to post weld smoothed root surface condition (Figure 19). The post weld smoothed root surface condition was obtained by mechanical grinding and final polishing of the root surface removing a superficial layer with a thickness of about 0.3mm assuring the removal of root defects. In fact reduced in-depth size of the root defect via surface smoothing increased the fatigue life in about 10X for a stress amplitude of about 80 MPa and R=0.1. Thus it is possible to conclude about the benefit of mechanical resistance when smoothing the root of FSW beads. Moreover FSW beads in smoothed condition shows a fatigue life close to BM results, most significantly for the lowest levels of stress amplitude. The results of FSW specimens in as welded condition are always better than the ones resulting from conventional welding solution: Synergic GMAW. The benefits of the fine equiaxial grain of the FSW nugget in fracture propagation phase plays an important role in this difference [26].

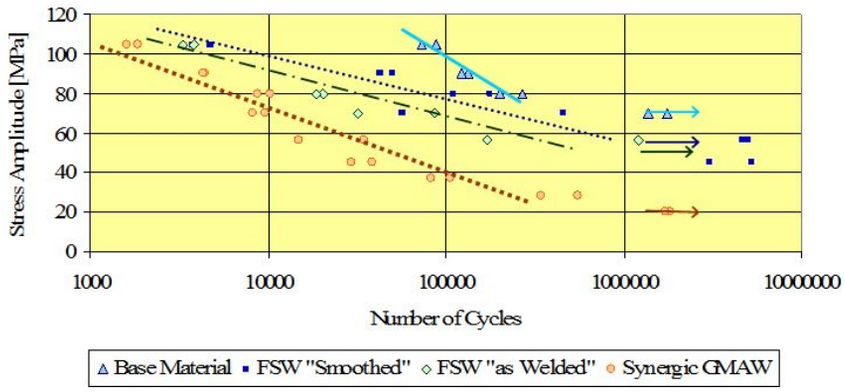

Figure 19. S-N curves from fatigue test trials (R=0.1; f=20Hz) of different testing conditions of AA5083-H111 (thickness = 4 mm).

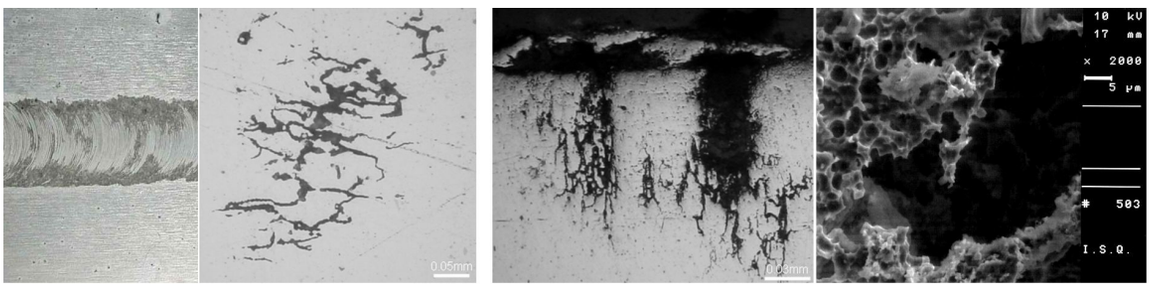

Figure 20. Corrosion developed in base material of AA5083-H111 after 7 days Exposition in Tagus River (20g/l NaCl). Exfoliation of the top surface of a FSW bead and intergranular corrosion along the Al-Mg precipitates resulting in pitting formation mechanism localized under the flash of the weld bead.

Several intergranular corrosion tests were performed for AA5083-H111 focusing the naval applications. These testes were implemented according to ASTM G67: Nitric Acid @ 30 ºC during 24hand also for 7 days of exposition to Tagus river water (20g/L NaCl) as depicted in Figure 20. The results show that the loss mass in the base material samples was much higher

http://dx.doi.org/10.5772/52026

than in the welded samples. This happens because intergranular corrosion mechanism was most susceptible at the intergranular precipitates and these were more abundant in base material. Exfoliation corrosion tests demonstrate that the corrosion resistance of the AA5083-H111 was better when better surface finishing was obtained for the weld bead. Thus, the higher roughness at the top of the weld bead promotes the earlier start and faster development of the corrosive attack [23].The typical geometrical discontinuities left by the shoulder on the top of FSW beads, namely: i) indentation and/or flash at advancing and retreating sides; and ii) semi-circular striates on the processed area under the shoulder, acts as preferential concentration points for the corrosive media. Root defects such as LOP also promote a faster and localized corrosion mechanism at this zone.

3.4. Advantages and limitations

The advantages claimed for the process include:

- Solid-phase nature of the process;
- Capability of welding materials whose structure and properties would be degraded by melting;
- Minimal edge preparation required;
- Machine tool technology, simple to use with good surface appearance;
- Minimal distortion;
- Hot forged microstructure;
- Low residual stress levels, compared with arc welding processes;
- Environmentally friendly with absence of welding fume and excessive noise;
- Suitability for automation;
- Good mechanical properties;
- Welding consumables not required, with exception for inserts that can be used and gas shielding for reactive materials such as titanium and its alloys;
- Not influenced by magnetic forces;
- Continuous - unlimited length;
- Joint can be produced from one side and in all positions.

The current limitations of the FSW process are:

- Backing anvil required (except bobbin stir);
- Keyhole at the end of each weld (except with the introduction of a run-off tab or when a FSW tool with a retractable probe is used);
- Not be able to start the weld joint from the start of the of the joint between the plates to be welded (except when using a run-on tab);

- Workpiece requires rigid clamping (except when the Twin-stir™ variant is used);
- Application not as flexible as certain arc welding processes.

3.5. The challenges in modelling the FSW

The development of computational models can greatly contribute to better understanding any industrial process, particularly FSW. A validated model has the potential to produce reliable information about the deformation and mixing patterns that are important when designing FSW tools and thus should be capable of producing welds free of defects and voids. Further, a model can measure process characteristics that are difficult to observe experimentally such as local strains, strains rates and stresses. These strain and stress fields, together with temperature histories are seen as critical in predicting microstructure evolution. A detailed understanding of microstructural evolution can guide FSW designs by further improving mechanical properties, fatigue strength and corrosion resistance.

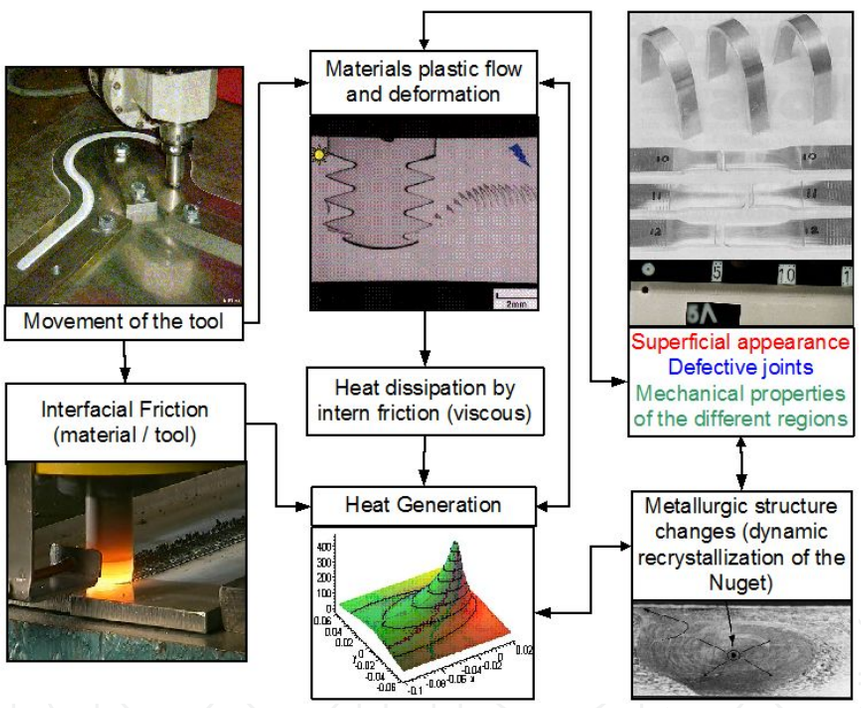

Figure 21. Coupled mechanical/thermal/metallurgical character of FSW process.

While considerable experimental work has been done to improve the knowledge on FSW, there's yet a lot of work needed to create a satisfying global model that can produce consistent results. The main difficulties in modeling FSW are [27]:

- Extensive material deformation in the region containing fully-plasticized material;
- The viscous-plastic flow imposed by the tool rigid surface, into the materials constrained by the interaction with the cold base material, with an essentially elastic behaviour, and the rigid plate (anvil) supporting the joint;

http://dx.doi.org/10.5772/52026

- Heat generated due to the sliding between the surface of the tool and the materials in the joint, depends on an unknown the friction coefficient;
- The correct prediction of the viscous-plastic flow imposed by the tool rigid surface into the materials being welded is also important because the viscous dissipation contributes significantly to the heat development during the performance of the weld bead;
- The materials thermo-mechanical properties vary throughout the FSW process;
- The thermal flow into the tool and support plate, needs to be considered in the models;
- FSW process modeling does not allow geometric simplification because it deals with a complex 3D material flow around the pin;
- The highly rotating tool pin has, typically, a complex geometric profile (e.g. threaded), which is rather difficult to consider for most of the numerical methods available.

The challenge is then to create a model able to fully describe the complex FSW process as illustrated in Figure 21.

4. Friction Stir Channeling

4.1. Fundaments of the process

Friction Stir Channeling (FSC) is an innovative solid-state manufacturing process able to produce continuous internal channels in monolithic plates in a single step. The channels can have any path and variable dimensions along the path. During FSC, a non-consumable rotating tool with a specific shoulder and probe profile is inserted into the solid block, or plate, where the channel is to be opened, and forced to traverse along a predetermined path, creating a fine grain recrystallized microstructure around the new channel. The FSC process results from the application of the correct combination between the direction of tool rotation and the orientation of the probe threads and shoulder scrolls. The following actions will be applied to the visco-plasticized workpiece material: i) an upward action directed to the shoulder, along the threaded probe, combined with ii) an outward/centrifugal action along aspiral scrolled shoulder.

The features of the channels produced with FSC can be controlled by selecting the processing parameters and tool geometry, e.g., during the FSC process, an upward force is generated by rotating a left-hand threaded tool counter-clockwise. The action of the tool produces the “third-body region”and forces part of this viscous material to flow out from the processing zone. Simultaneously, the FSC tool closes the top of the processed zone via the action of the shoulder, enabling the creation of a continuous internal channel. The Figure 22 shows a schematic representation of the FSC process [28].

The FSC process was firstly proposed as a method of manufacturing heat exchanging devices. The applicability of the FSC concept have been discussed and demonstrated in [7,29] to create continuous channels along linear and curved profiles, as well as the possibility of

manufacturing mini channel heat exchangers (MCHX). The FSC process was initially based on converting one possible defect in FSW: the formation of internal continuous voids, into a manufacturing technique where all the material extracted from the metal workpiece laid over the processed zone bellow the shoulder [29], within a clearance between the shoulder and the metal workpiece.

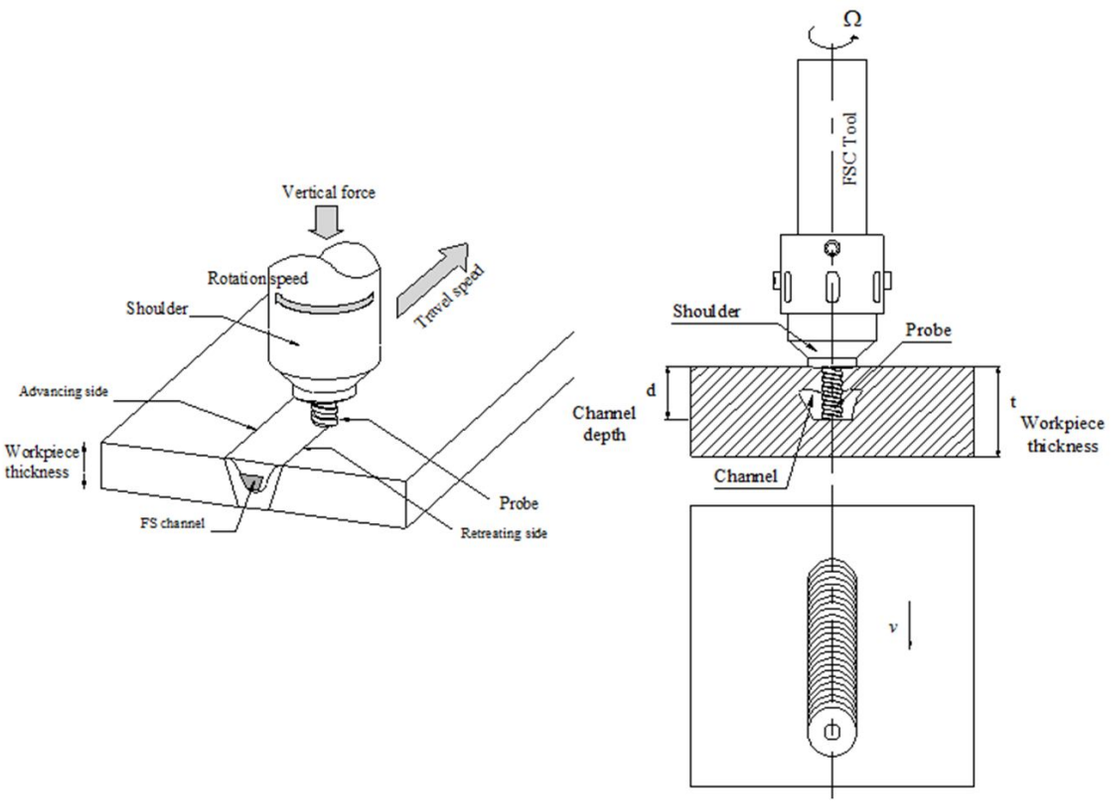

Figure 22. Schematic representation of the FSC process fundaments: parameters and viewsof the cross-section and plan.

There is a study [30] presenting a model based on the flow partition deformational zones for defect formation during FSW. The occurrence of voids in the FSW nugget has been attributed to defective material flow mainly because of the non-optimal processing conditions or geometry of the tool features. The model applies the principle of mass balance to address void formation in the nugget.

A recent development made by the authors of the present chapter and proposed in [31] allows to promote distinct material flow, where a controlled amount of material from the metal workpiece, flow out from the processed zone producing the internal channel. Thus, the material flowing from the interior of the solid metal workpiece is not deposited on the processed surface but flowed outside from the processed zone in the form of flash self-detachable or easy to extract. The position and size of the channels can therefore be controlled and the processed surface can be left at the same initial level. It is also possible to integrate in the tool, a surface finishing feature [31].

http://dx.doi.org/10.5772/52026

The high flexibility and low production costs of this innovative manufacturing process provide this technology a great potential to be successfully introduced in various industries. However, FSC still need to have a considerable development to prove its industrial applicability.Recent advances of tooling for FSC [28] shown to be possible to control during FSC the processed surface finishing and position. The high level of adaptability of FSC makes it possible to apply to many different technical field domains and can bring significant advantages for already existent and new industrial applications.Meanwhile some aluminum alloys have already been subjected to FSC, e.g.: 5 mm thick plates of AA6061-T6 [29], 13 mm thick plates of AA7178-T6 and 15 mm thick plates of AA5083-H11 [32].

The Figure 23 shows a representation of a typical cross section of a channel from FSC with the identification of the advancing and retreating sides and depicting the main microstructural regionsin the vicinity of the channel, namely: i) nugget; ii) TMAZ; iii) HAZ, and iv) BM.

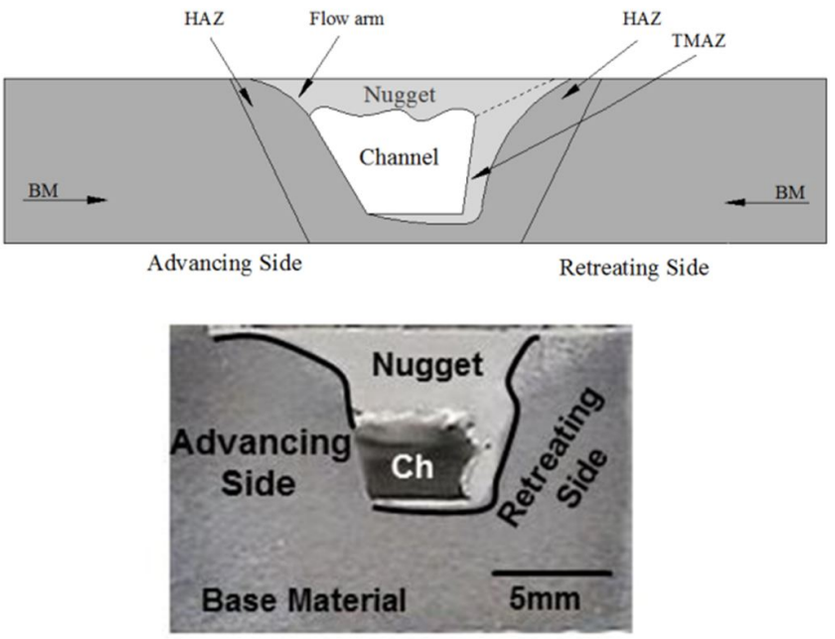

Figure 23. Typical cross section macrograph of a friction stir channel including the main microstructural regions.

4.2. Parameters of the process

Because the FSC is based on the same principles of FSW, the parameters type and the process control in FSC, via position/vertical downward force criteria, are essentially the same of the FSW process. Understanding the material flow, process forces and metallurgy is therefore necessary to control and optimize the channel formation to ensure its industrial successful application.

In order to optimize the friction stirred channels components' performance, and considering that the channel formation is sensitive to FSC parameters variations, it is important to identi-

fy, understand and establish interactions between the processing parameters. Some know-how is already possible to establish:

- The probe and shoulder geometry defines the material removed from the interior of the metal workpiece. The material at the "third-body region" is brought against the shoulder by the probe and moved outside by the spiral striate(s) of the shoulder as result of the combination between the i) orientation and geometry of the threads on the probe; ii) orientation and geometry of the shoulder striate(s); iii) direction of tool rotation and iv) remaining process parameters;
- The position of the advancing side and bottom of the channel (channel's depth) are prescribed and well controlled by the shape and position of the probe within the monolithic workpiece material. These surfaces present relative smooth finishing;
- The channel ceiling and retreating side present rough finishing and their position is controlled by the process parameters. Thus, by tuning the parameters it is possible to establish the section of the channel and optionally continuously change this section during the FSC process;
- The shoulder is responsible for constraining the deformed material, closing the ceiling of the channel and its scrolls for driving away a controlled amount of material from the interior of the metal workpiece to outside, in the form of flash;
- If the parameters are correct, the amount of material brought against the shoulder by the probe is equal to the amount of material removed outside by the shoulder;
- If the shoulder is plan and smooth (i.e., not scrolled), the material pushed out by the probe features is deposit underneath the shoulder, at the inherent gap between the shoulder and the workpiece;
- The tool rotation and travel speed control the amount of visco-plastic flow and subsequent heat generation from frictional dissipation during the process. These two parameters, along with plunge depth, if the process is performed via position control, affect the axial force applied on workpiece, which significantly affects the overall channel quality;
- The operating conditions for which the process is more stable and produce better results are cold conditions;
- The FSC parameters are not directly transferable from one aluminum alloy to another, the workpiece material thickness and the thermal conductivity of materials in contact with the workpiece, like anvil and clamping system, influence the cooling rate and the temperature gradients through thickness. Also the heat cooling system of the tool and dissipation through the spindle can influence the process and the tool lifetime.

4.3. Tool features and development

In the FSC tool the probe and shoulder geometry are the most important features that influence the channel formation, shape, localization and properties. The initial FSC studies conducted in [29] used a cylindrical threaded probe with a diameter of 5 mm and 4 mm length

http://dx.doi.org/10.5772/52026

and with an initial clearance between the shoulder and the metal workpiece, where the material from the base of the probe is deposited. Since that time, developments have been made by the authors of present chapter [28,31,32], allowing to promote a distinct material flow, discarding the need for a gap between the shoulder and the original surface of the workpiece. At the actual state of the art, with the correct set of parameters there is no need of further finishing operations, but if any is demanded, the actual shoulder design has advanced to geometries capable to integrate a surface finishing feature, and then processed surface can always be left at any required final level, simultaneously with the FSC process, and it is not require to perform a further finishing process. Figure 24 shows the modular FSC tool concept developed [31].

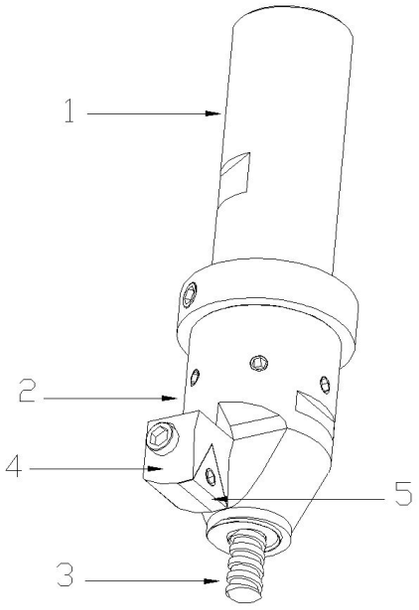

Figure 24. – 3D view of a modular FSC tool. (1) tool body, (2) shoulder, (3) probe, (4) cutting insert clamping, (5) cutting insert.

Resulting from experimental tests, it was established [31] that the number of cutting inserts might have the same that the number of the shoulder spirals striates as shown in Figure 25.

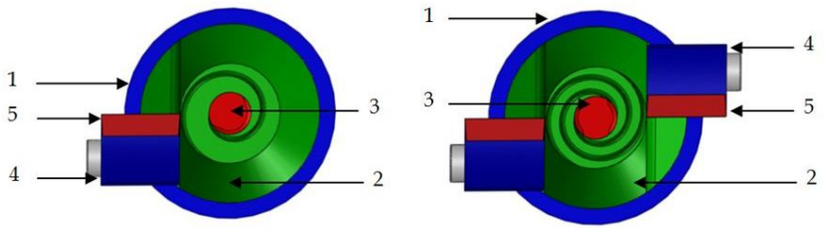

Figure 25. Top view sections showing the equality between the number of scrolls and the number of cutting inserts on the shoulder. (1) tool body, (2) shoulder, (3) probe, (4) cutting insert clamping, (5) cutting insert.

Initially, the FSC tool's components were made of the same material typically applied in FSW: AISI H13, however this material has shown not to be the most appropriate to produce the probes to perform FSC on aluminium alloys at depths greater than 10 mm from the metal workpiece surface. Developments are being made, namely the study of new probe materials and designs, in order to increase the tool's life. Conical probes have long lives comparing to cylinders ones but cylinders probes are more efficient than conical for this technological process which the main objective is to extract material from the metal workpiece.

4.4. Advantages and limitations

The following advantages can be established for the innovative solid-state manufacturing FSC process:

- Able to produce continuous free path internal channels in monolithic plates in a single step;
- The channels can have variable positioning and dimensions along the path;
- The channels have good dimensional stability and repeatability;
- Recent advances of tooling for FSC shown to be possible to control the surface finishing and position of the exterior processed surface, during the execution of the process;
- Capability of producing highly efficient conformal cooling/heating channels. FSC process also has the capability to produce cooling/heating systems in a single component whereat no time is loss joining components;
- The high level of adaptability of FSC makes it possible to apply to many different technical field domains and can bring significant advantages as alternative of already existent technologies, such as, drilling, EDM and milling;
- Environmentally friendly process using a no consumables.

The current limitations of the FSC process are:

- At the actual state of art, the non-consumable tool lifetime is small because of premature fracture under the complex and demanding fatigue loading;
- Sensitivity to change of parameters;
- To produce channels by FSC access from one surface of the metal workpiece is required;
- A residual hole is left open at the end of the channel path.

4.5. Geometric and metallurgical characterization of the channels

The shapes of the channels obtained from FSC are closer to a parallelogram. The channel shape varies with the process parameters. Figure 26 shows the variation of the shape of the channel with changing the FSC process parameters.

The channel geometry can be attributed to the volume of processed material that is displaced out of the "third-body region" by the FSC toolper unit of rotation and also the com-

http://dx.doi.org/10.5772/52026

pacting force that is applied on the channel ceiling during the travel forward movement by the rotating shoulder. The upper surface of the channel (channel ceiling) is rough and wave shape and the channel advancing side (shear side) does not exhibit any significant roughness comparing to the retreating one. The bottom of the channel is relatively smooth and flat due to the flat nature of the tool probe base (Figure 27).

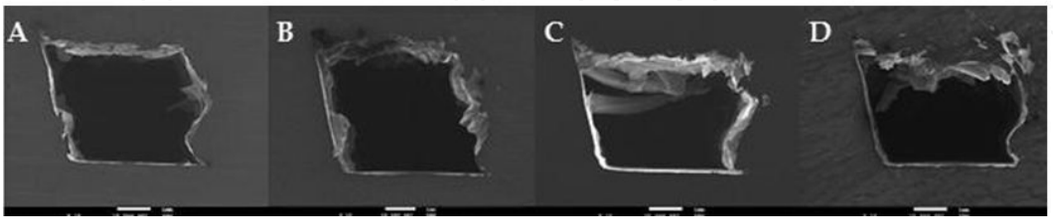

Figure 26. Cross section macrograph showing the channel geometry at different FSC processing parameters for the same FSC tool: a) 600 rpm, 80 mm/min.; b) 600 rpm, 150 mm/min.; c) 800 rpm, 80 mm/min. and d) 800 rpm, 150 mm/min.

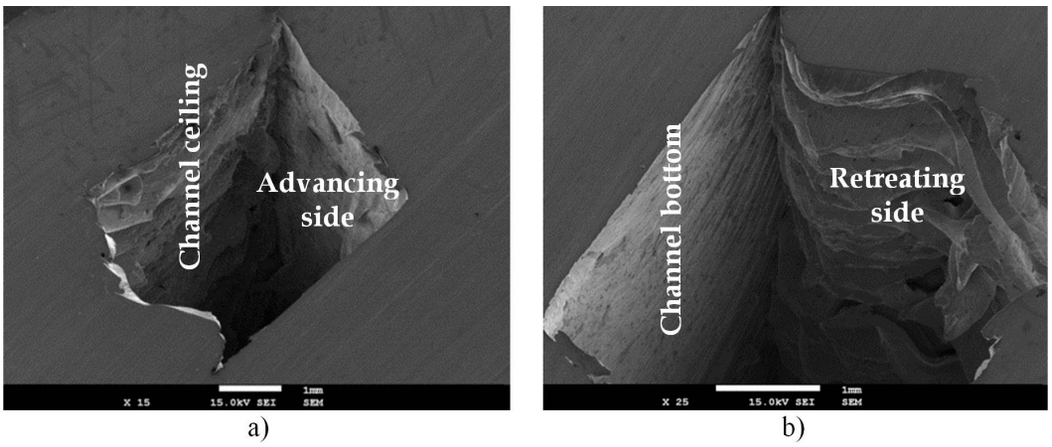

Figure 27. Cross section of a channelshowing the roughness: a) on the ceiling and on the advancing side; b) on the bottom and on the retreating side.

The Figure 28 shows a cross section of a friction stir channel produced with a tool rotation speed of 800 rpm and a tool travel speed of 80 mm/min. In the macrograph depicted in Figure 28 three main regions are visible: i) channel; ii) stir zone (nugget), and the iii) unprocessed base material. The channel nugget (Figure 28b) presents a fine equiaxed recrystallized grain, with a tail heading to the shoulder periphery, at the advancing side (Figure 28c).In details “a)”, “c)” and “d)” of Figure 28 it is possible to identify an additional layer surrounding the nugget, referred to as a thermo-mechanically affected zone (TMAZ). Due to tool rotation and linear movement combination, the probe shears the material from the advancing side and flows it around the retreating one, resulting in an asymmetric processed zone. It can be observed in details “e)” and “f)” in Figure 28 that the stir zone (nugget) is more extensive in the retreating side than in the advancing one. The Figure 29, present the hardness field measured in the same cross-section presented in Figure 28.

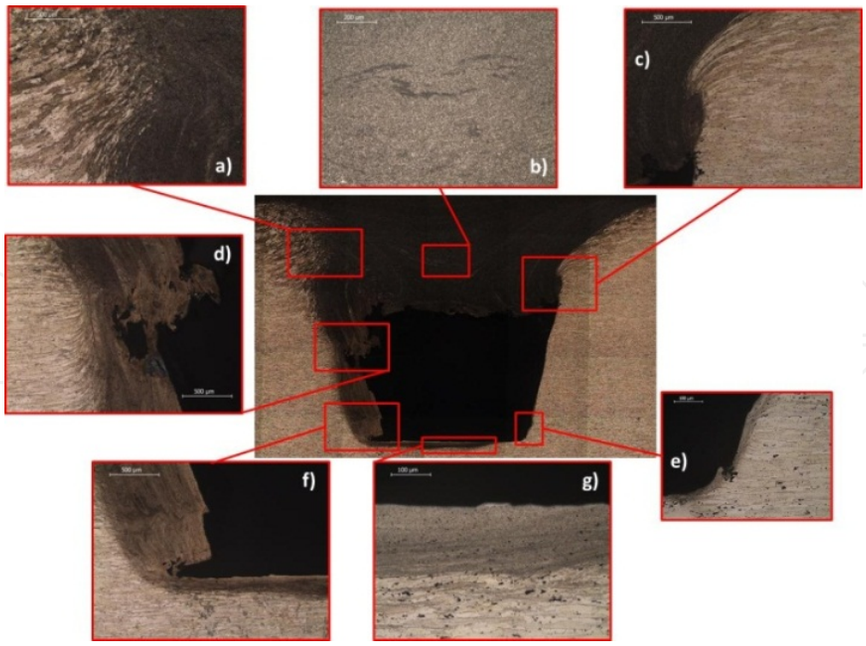

Figure 28. Metallographic results of a cross section at the vicinity of a channel produced with FSC: Ω= 800 rpm and v = 80 mm/min.

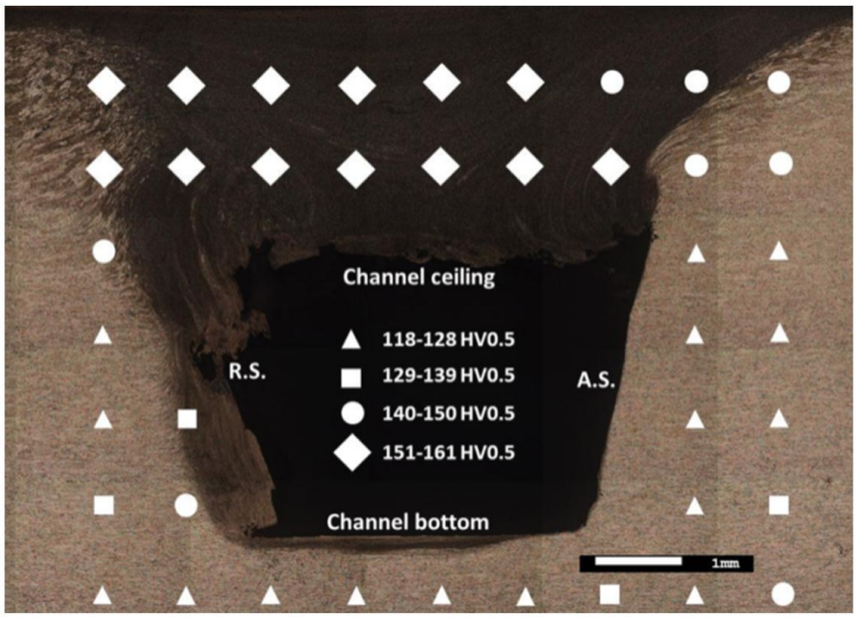

Figure 29. Hardness field in the vicinity of a channel produced with FSC: = 800 rpm and v = 80 mm/min.

In order to standardize the characteristics of the channel shape and to spot possible trends in the channel shape change with the variation of the process parameters, three geometrical parameters of the channel were establish in Figure 30:

- Channel area;

http://dx.doi.org/10.5772/52026

- Closing layer thickness (D);
- Shear angle (α).

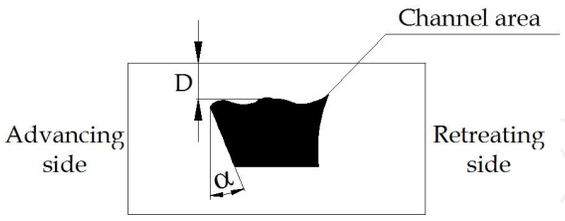

Figure 30. Schematic representation of a cross-section view of a friction stirred channel workpiece showing the geometrical parameters closing layer thickness (D) and shear angle (α).

Results presented in [28] shown that the closing layer thickness values are consistent with those obtained for the channel area, i.e., as the channel area increases, the closing layer thickness decreases. But on the other hand, the shear angle has no relationwith the values of channel areas or even with the closing layer thicknesses for the different FSC conditions.

4.6. New tests for characterization of the channels

Despite the similarities between FSC and FSW processes, some of the testing techniques and criterions typically applied to the inspection and characterization of weld joints properties make no sense to be directly applied to FSC, e.g., direct comparison of mechanical properties of welded specimens with similar base material properties. In order to assess the quality of the channels for different paths, procedures are proposed to assess the quality of FSC results for slop and spiral paths.

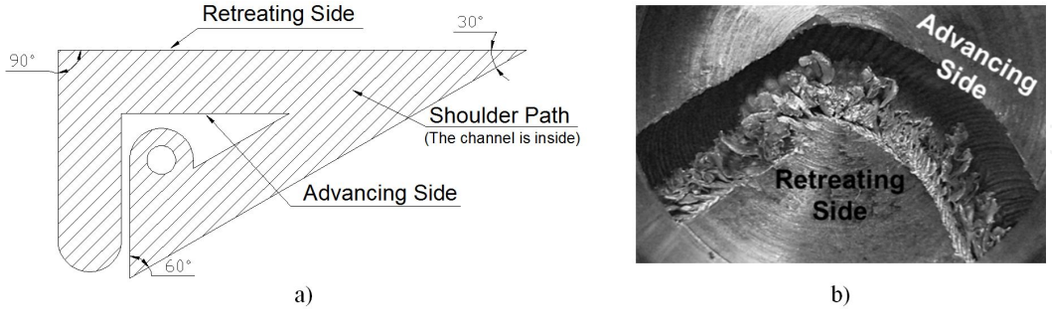

Figure 31. Slope paths. a) linear sloped path tested and b) result of the visual inspection after milling a hole at the 90 degree corner.

For linear sloped paths, namely for the closed ones (Figure 31a), the path should be carried out in order to the retreating side stays outside and the advancing side inside the path. The path presented allows assessing continuous channels with variations of 30, 60 and 90 degrees along its path. Linear sloped paths corners should be inspect. As a procedure, it is proposed milling the FSC plate of the non-processed side to the channel bottom using a milling

cutter with the same diameter than the FSC tool shoulder. The result of applying this procedure to the 90 degree corner is shown in Figure 31b.

Such as for linear sloped paths, the spiral paths should be carried out in order to the retreating side stays outside and the advancing side inside the spiral. The minimum allowed gap between spirals is the shoulder radius. To assess the geometrical stability of channels during spiral paths two cuts are recommending: a horizontal cut through the transition points of the arcs and a vertical cut through the outermost points of each arc as shown in Figure 32. Made the cuts, the channels cross sections should be assessed, e.g., according to the geometrical parameters presented in Figure 30.

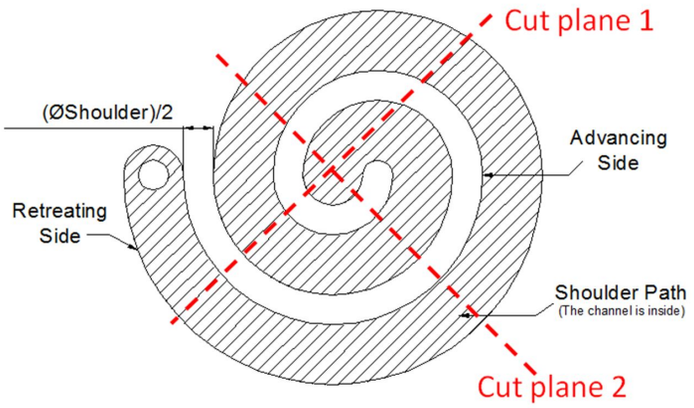

Figure 32. Schematic representation of the spiral path produced showing the minimum allowed gap between spirals (shoulder radius).

In order to evaluate the mechanical strength of the FSC processed zone, a free-bend test is proposed as a FSC performance parameter. The proposal is to analyse the mechanical strength of a large area, the FSC processed zone, rather than a specific and small zone as the welded joints root in FSW. In Figure 33 is shown the 4 points free-bend tests results for four specimens tested which were extracted from the same trajectory of an unstable FSC procedure. From Figure 33 it is possible to verify, that the channel strength is not constant over the path. The friction stir processed zone is more resistance at the beginning of the path than at the end. All specimens tested fractured at the advancing side, namely in the boundary between the nugget and the thermo-mechanically affected zone.

To obtain the indentation resistance of the processed zone with FSC, the authors also propose aMacro indentation resistance test. Thus, specimens with a transversal channel should be produced according to the following dimensions: i) Length ≥7×∅Shoulder; ii) Width= 2×plate thickness; iii) Depth =plate thickness. The specimens should betested according to the apparatus presented in Figure 34. The friction stir processed zone must be in contact with the mandrel. The mandrel diameter must be equal to the probe maximum diameter. It is recommend a mandrel velocity about 1mm/min. The test ends when the maximum force is reached.

http://dx.doi.org/10.5772/52026

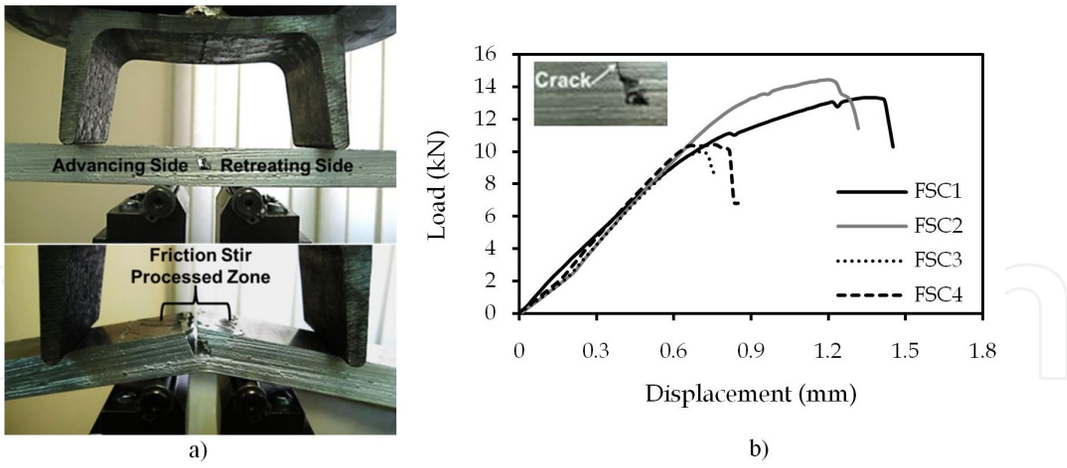

Figure 33. Points free-bend tests for FSC: a) schematic representation of the standard E 290-97a suited for testing FSC specimens 4pt bending resistance and b) experimental results.

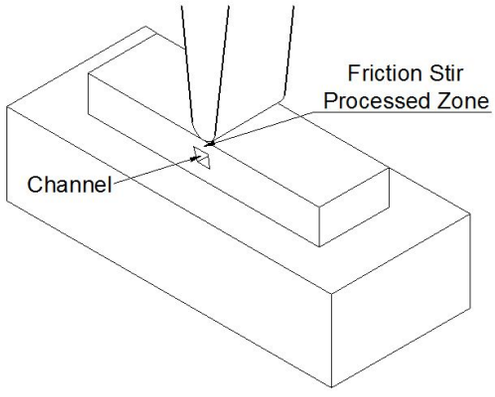

Figure 34. Macro indentation resistance test apparatus.

Because friction stir channels have high potential application in heat exchanger industry and in conformal cooling/heating systems, it is crucial to assess effective air tightness and their mechanical resistance when loaded with internal pressure (in Figure 35, it is proposed an internal hydraulic pressure test). For these tests, it should be produced parallelepiped specimens with the friction stir processed zone centered and according to the following dimensions: i) Length≥5×∅Shoulder; ii) Width =2×∅Shoulder; iii) Depth =plate thickness.

To assess the channels' airtightness should be used pressurised helium (at a minimum of 5 bar) because the helium atom is the smallest among the inert gases and thus, it is possible to ensure that any cracks greater than the helium's atom is detected. In order to see the released gas, the specimen should be immersed in a container with clean water.

Relatively to the internal hydraulic pressure tests, they were carried out using an oil pressing machine and a 100 bar manometer. Themanometerusedshould bewhich ensuresthe FSC system design requirements.

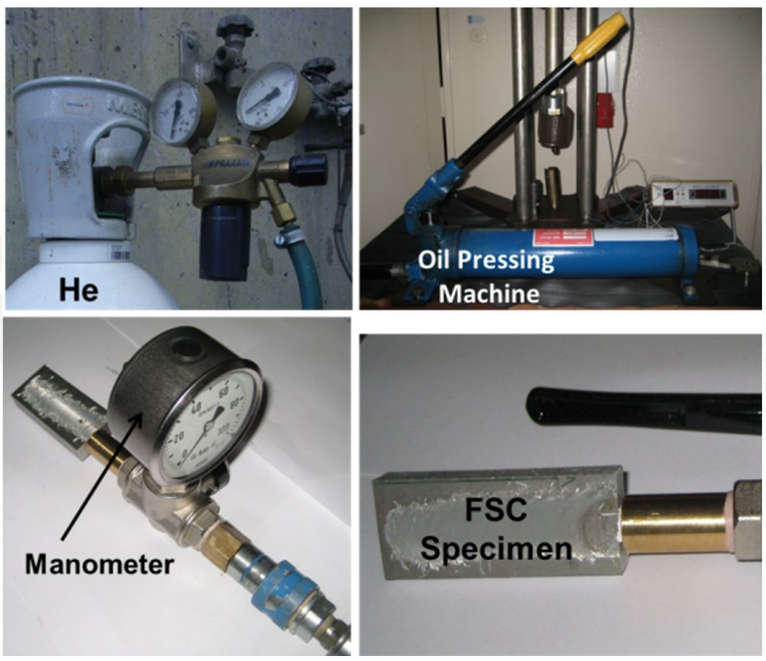

Figure 35. Airtightness and internal hydraulic pressure tests apparatus.

4.7. Establishment of potential applications

The value of a technology is directly related with the amount of solutions and add-value it can provide to the industry. Consequently, if a new technology is being developed it is of major importance to analyse what are the possible industrial applications it has.

The generation of a continuous channel by FSC has the potential to open a wide range of applications, such as, conformal cooling/heating systems, heat exchangers and advanced tailored performance engineering metallic materials.

Conformal cooling is a concepton which the refrigerating channels follow the configuration of the part shape, enabling higher quality and productivity in the cooling/heating procedure. The influence on the cooling time and surface quality is significant and this concept has been growing recently. The FSC process is able to produce these conformal channels.

A prototype was developed for a company producing plastic injection moulds to demonstrate the potential of FSC technology (Figure 36). The prototype was discussed with the company, to determine if it could be an alternative to produce small dimension channels for thermoplastic parts that are produced by mould injection. These moulds have cooling channels behind the part surface that defines the geometry of the part. Owing to the complex geometries of certain components, FSC could be the solution for these channels due to the flexibility of the technology that permits the channels to have any desired path and position within the mould.

The generation of a continuous channel by FSC has the potential to open a wide range of applications also in heat exchanger industry.Compact heat exchangers are generally used in

http://dx.doi.org/10.5772/52026

industry, especially in gas-to-gas or liquid-to-gas heat exchangers. For example, vehicular heat exchangers, condensers and evaporators in air-condition and refrigeration industry, aircraft oil-coolers, automotive radiators, and intercoolers or compressors and FSC has the ability to produce the channels for any of these types of heat exchangers, which demonstrates the elevated applicability it has in the various industries [7].

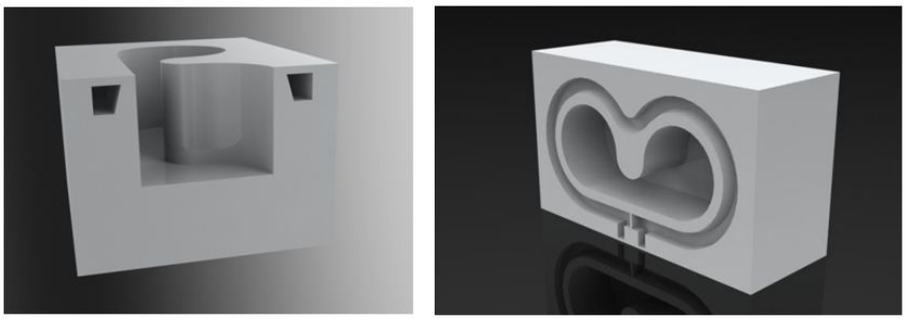

Figure 36. Sample of a prototype developed for a mouldcompany with a conformal cooling channel produced by FSC.

A new application, in development, is the production of Advanced Tailored Performance of Engineering Metallic Materials (ATEM) by FSC. A predetermined friction stirred channel pattern is produced in an aluminum workpiece in order to obtain a component with specific mechanical and metallurgical properties. FS channels can be filled with other materials or be used only to reduce the component structural weight and optimize is stiffness as illustrated in Figure 37. The channels produced with FSC, can also be used for crossing wires within solid components with many potential application for aluminium alloys structures, namely in aeronautics.

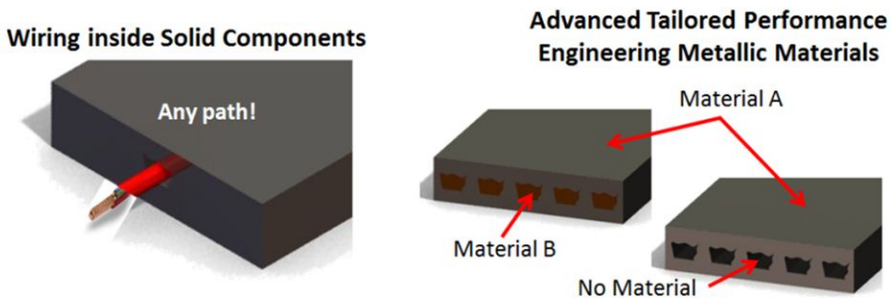

Figure 37. Schematic illustration of two alternative industrial applications with internal channels produced by FSC.

5. Conclusions

From the present work the following conclusions can be drawn:

- Three relevant friction based processing processes covering a wide range of technological applications are presented in it state of the art fundaments and main features. Also, the most significant experimental results are depicted;
- The concept supporting all the three processes addressed in the present chapter, and many others processes on the field of solid state processing, is the material flow within open or closed "third-body region". This concept is introduced in some detail in order to allow readers to be able to further develop the actual solutions and invent new ones;
- The Friction Surfacing (FS) process is a lean coating technology ideal for localized surface engineering applications, requiring the joining of materials with compatibility issues. As a solid state process, there is no melting involved and the coating material is solely provided by a consumable rod. Friction surfacing produces high strength coatings, soundly bonded, with low dilution, no porosity and little part distortion, making FS suitable to process thermal sensitive materials, such as, aluminium alloys. The absence of splashes, toxic fumes and radiation makes friction surfacing a cleaner alternative. However, bonding quality at coating edges need further evolution and post processing is generally required to obtain uniform coating surface and remove the poorly bonded portions;
- The basic fundaments of friction stir welding (FSW) process have been presented. These basic fundamentals have enabled the invention and development of many variants of FSW. FSW is a mature and reliable technology with guidelines in many construction codes, mainly focusing on products made from aluminium and its alloys. The new ISO standard 25239 Friction stir welding - Aluminium alloys, has been published. This ISO standard will help with the implementation of FSW technology in light metal fabrication industries. Moreover, the FSW is a very complex process and difficult to be assessed based on computational modeling;
- The Friction Stir Channeling (FSC) process is a disruptive innovation enabling higher efficiency in energetic applications and advances of structural design of many products. With this chapter the authors proposed new feasible FSC performance parameters based on non-conventional testing techniques, some quantitative and others qualitative. The FSC performance parameters proposed to assess the tightness are based on the amount of material removed, the macro indentation resistance of the FSC processed zone, the bending resistance of the FSC processed surface under tensile stress and the geometrical stability of channels during linear and spiral FSC paths.

Acknowledgements

The authors would like to acknowledge FCT/MCTES funding for the project FRISURF' (PTDC/EME-TME/103543/2008) and PhD grants: SFRH/BD/62963/2009 and SFRH/BD/78539/2011.

http://dx.doi.org/10.5772/52026

Author details

Pedro Vilaça[1,2*], João Gandra[2] and Catarina Vidal[2]

*Address all correspondence to: pedro.vilaca@ist.utl.pt

1 IDMEC, Instituto de Engenharia Mecânica, Lisbon, Portugal

2 IST-UTL, Instituto Superior Técnico, Lisbon, Portugal

References

[1] Vilaça, P. (2003). Fundaments of Friction Stir Welding Process- Experimental Analysis and AnalyticalModeling. *PhD Thesis*, Technical University of Lisbon.

[2] Vilaça, P., Pepe, N., & Quintino, L. (2006). Metallurgical and Corrosion Features of Friction Stir Welding of AA5083H111. Welding in the World. , 50(9/10), 55-64.

[3] Leitão, C., Leal, R. M., Rodrigues, D. M., Loureiro, A., & Vilaça, P. (2009). Mechanical Behaviour of Similar And Dissimilar AA5182H111 And AA6016-T4 Thin Friction Stir Welds. *Materials and Design*, 30, 101-108.

[4] Thomas, W. M. (2009). An Investigation and Study into Friction Stir Welding of Ferrous-Based Material. *PhD thesis*, University of Bolton.

[5] Klopstock, H., & Neelands, A. R. (1941). An Improved Method of Joining or Welding Metals. *Patent application Nº 572789*.

[6] Thomas, W. M., Nicholas, E. D., Needham, J. C., Murch, M. G., Temple-Smith, P., & Dawes, C. J. (1991). Improvements relating to friction stir welding. *US Patent Nº. 5460317*.

[7] Mishra, R. S. (2005). Integral Channel in Metal Components and Fabrication Thereof. *US Patent Nº 6923362*.

[8] Bedford, G. M., Vitanov, V. I., & Voutchkov, I. I. (2001). On The Thermo-Mechanical Events During Friction Surfacing of High Speed Steels. *Surface and Coatings Tecnhology*, 141-34.

[9] Nicholas, E. D., & Thomas, W. M. (1986). Metal Deposition by Friction Welding. *Welding Journal*, 8-17.

[10] Shirzani, A. A., Assadi, H., & Wallach, E. R. (2001). Interface Evolution And Bond Strength When Diffusion Bonding Materials With Stable Oxide Films. *Journal of Surface and Interface Analysis*, 31-609.

[11] Batchelor, A. W., Jana, S., Koh, C. P., & Tan, C. S. (1996). The Effect of Metal Type and Multi-Layering on Friction Surfacing. *Journal of Materials Processing Technology*, 57-172.

[12] Chandrasekaran, M., Batchelor, A. W., & Jana, S. (1997). Friction Surfacing of Metal Coatings on Steel and Aluminum Substrate. *Journal of Materials Processing Technology*, 72-446.

[13] Vitanov, V. I., Voutchkov, I. I., & Bedford, G. M. (2000). Decision Support System To Optimize The Frictec (Friction Surfacing) Process. *Journal of Materials Processing Technology*, 107-236.

[14] Macedo, M. L. K., Pinheiro, G. A., Santos dos, J. F., & Strohaecker, T. R. (2010). Deposit By Friction Surfacing and its Applications. *Welding International*, 24-422.

[15] Nicholas, E. D. (1993). Friction Surfacing. ASM Handbook- Welding Brazing and Soldering. *ASM International*, 6, 321-323.

[16] Rafi, H. K., Ram, G. D. J., Phanikumar, G., & Rao, K. P. (2011). Microstructural Evolution During Friction Surfacing of Tool Steel H13. *Materials and Design*, 32-82.

[17] Gandra, J., Miranda, R. M., & Vilaça, P. (2012). Performance Analysis of Friction Surfacing. *Journal of Materials Processing Technology*, 212-1676.

[18] Seidel, T. U. , & Reynolds, A. P. (2011). Visualization of the Material Flow in AA2195 Friction-Stir Welds Using a Marker Insert Technique. *Metallurgical and Materials Transactions A.*, 32(11), 2879-2884.

[19] London, B., Mahoney, M., Bingel, W., Calabrese, M., & Waldron, D. (2001). Experimental Methods for Determining Material Flow in Friction Stir Welds. Japan. *3rd International Symposium on Friction Stir Welding*.

[20] Vilaça, P., Quintino, L., Jorge, F., & Santos, . (2005). dos. iSTIR- Analytical Thermal Model for Friction Stir Welding. *Journal of Materials Processing Technology*, 169(3), 452-465.

[21] Leitão, C., Leal, R. M., Rodrigues, D. M., Vilaça, P., & Loureiro, A. (2008). Material flow in Friction Stir Welding. *Journal of Microscopy and Microanalysis*, 14(S3), 87-90.

[22] Leal, R. M., Leitão, C., Loureiro, A., Rodrigues, D. M., & Vilaça, P. (2008). Material Flow in Heterogeneous Friction Stir Welding of Thin Aluminium Sheets: Effect of Shoulder Geometry. *International Journal of Materials Science and Engineering A*, 498(1/2), 384-391.

[23] Vilaça, P., Pepe, N., & Quintino, L. (2006). Metallurgical and Corrosion Features of Friction Stir Welding of AA 5083H111. *Welding in the World*, 50(9/10), 55-64.

[24] Vilaça, P., & Quintino, L. (2006). Experimental and Computational Developments of FSW. Welding. *Equipment and Technology*, XVII, 17-24.

http://dx.doi.org/10.5772/52026

[25] Santos, T., Vilaça, P., Reis, L., Quintino, L., & Freitas, M. (2008). Advances in NDT Techniques for Friction Stir Welding Joints of AA2024. New Orleans, USA. *The Minerals, Metals & Materials Society (TMS) 2008 Annual Meeting & Exhibition*, 3, 27-32.

[26] Pépe, N., Vilaça, P., Quintino, L., Reis, L., & Freitas, M. (2006). Fatigue Behavior of Shipbuilding Aluminium Alloy Welded by Friction Stir Welding, Session 3: Welds. Atlanta, USA. *9th International Fatigue Congress*.

[27] Santos, T., Vilaça, P., Quintino, L., Dos, J., & Santos, . (2009). Computational Tools for Modeling FSW and an Improved Tool For NDT. *Welding in the World*, 53(5-6), r99r108.

[28] Vidal, C., Infante, V., & Vilaça, P. (2012). Mechanical Characterization of Friction Stir Channels under Internal Pressure and In-Plane Bending. *Key Engineering Materials*, 105-108.

[29] Balasubramanian, N., Mishra, R. S., & Krishnamurthy, K. (2009). Friction Stir Channelling: Characterization of the Channels. *Journal of Materials Processing Technology*, 209-3696.

[30] Arbegast, W. (2008). A Flow-Partitioned Deformation Zone Model for Defect Formation During Friction Stir Welding. *Scripta Materialia*, 58-372.

[31] Vilaça, P., & Vidal, C. (2011). Modular Adjustable Tool and Correspondent Process for Opening Continuous Internal Channels in Solid Components. *National patent pending Nº 105628 T*.

[32] Vidal, C., Infante, V., & Vilaça, P. (2011). Mechanical Characterization of Friction Stir Channels Under Internal Pressure and In-Plane Bending. Dubrovnik, Croatia. *10th International Conference on Fracture and Damage Mechanics*.

IntechOpen